

AD-A115 298

NAVAL OCEAN RESEARCH AND DEVELOPMENT ACTIVITY NSTL S--ETC F/G 17/1

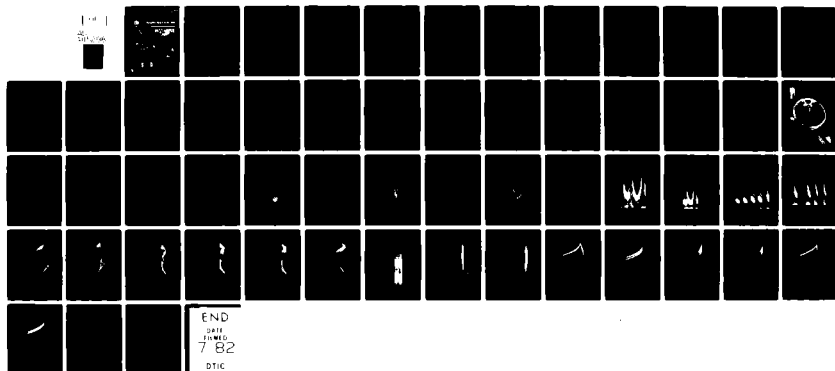
NAVIGATION HAZARD SURVEY SONAR.(U)

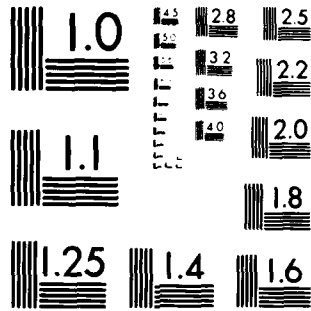
APR 82 6 J MOSS

UNCLASSIFIED

NORDA-TN-53

NL





MICROCOPY RESOLUTION TEST CHART  
NATIONAL BUREAU OF STANDARDS 1963-A

13

Naval Ocean Research  
and Development Activity  
NORL Station, Mississippi 39629



# Navigation Hazard Survey Sonar

AD A115298



DTIC  
ELECTE  
JUN 1982

Surge J. R. R. R.

Ocean Technology Division  
Ocean Science and Technology Laboratory

April 1982

**DISTRIBUTION STATEMENT A**  
Approved for public release;  
Distribution Unlimited

82-08-00-000

ABSTRACT

A towed side-scan sonar with a 2 nautical mile (nm) range would permit a hydrographic survey ship to sweep a 4 nm swath for navigation hazards. The increased track spacing made possible by such a system would result in substantial savings in ship time.

A conical, rather than a fan-shaped, beam would be required in coastal waters because of the proximity of the ocean surface and floor relative to the sonar range. For isovelocity water with sufficient wave height to make insonification of the surface undesirable, a 2.5° beam would be required for a 2 nm range in 80 meter (m) deep water, or for a 1 nm range in 50 m deep water.

The water depth required under refracting conditions depends on the mixed layer sound speed gradient and the surface wave height.

Nonlinear acoustics can be used to generate the required narrow beams at frequencies compatible with the 2 nm range without the use of excessively large projectors.

A feasibility demonstration experiment was performed at Seneca Lake under isothermal conditions. A transducer with a 0.9 m aperture was rotated in azimuth and excited parametrically in the 13-20 kHz region. Side-scan sonar imagery could be obtained to a range of 3.8 nm. Large features, such as shorelines, points, and underwater ridges, showed up best with 10 millisecond CW pulses. Small features such as sand steps and manmade objects showed up best with replica correlation signal processing.

Accession For	
NTIS GRA&I	<input checked="" type="checkbox"/>
DTIC TAB	<input type="checkbox"/>
Unannounced	<input type="checkbox"/>
Justification	
By	
Distribution/	
Availability Codes	
Dist	Avail and/or Special
A	



#### ACKNOWLEDGEMENTS

The author is indebted to Mr. William Konard and Dr. Mark Moffett of the Naval Underwater Systems Center for reports, data, and advice related to the calculation of nonlinear acoustics source levels and beam widths; to Mr. William Konard and Mr. Lynn Carlton of the Naval Underwater Systems Center for providing transducers, hydrophones, and electronic equipment, and for setting up and operating the experimental apparatus; the personnel at the Seneca Lake Sonar Test Facility for their support during the feasibility demonstration experiment; and Mr. Eigo Hashimoto of the NORDA Numerical Modeling Division for the sound speed profiles. The work was supported by the Defense Mapping Agency.

## CONTENTS

LIST OF ILLUSTRATIONS	iv
I. INTRODUCTION	1
A. BACKGROUND	1
B. ALTERNATE APPROACHES	2
II. BEAM PATTERN CONSIDERATIONS	3
III. NONLINEAR ACOUSTICS	6
IV. SOURCE PERFORMANCE PREDICTION	6
A. SOURCE LEVEL	6
B. BEAMWIDTH	7
C. SOURCE DESCRIPTION	7
V. FEASIBILITY DEMONSTRATION EXPERIMENT	7
A. APPARATUS	7
1. PULSED CW OPERATION	8
2. CORRELATION OPERATION	8
B. EDGE-ON FREQUENCY RESPONSE	9
C. BEAM PATTERNS	9
D. PULSED CW OPERATION	10
E. CORRELATION OPERATION	11
F. SUMMARY OF EXPERIMENTAL RESULTS	12
VI. REFRACTION	12
VII. SUMMARY AND RECOMMENDATIONS	13
VIII. REFERENCES	15

## ILLUSTRATIONS

Figure 1:	Geometry for Calculation of Required Beam Width	16
Figure 2:	Lower Bound on Required Beam Width for Constant Depth Isovelocity Water	17
Figure 3:	Sea Surface Backscatter Strength Resulting from Beam Widths in Excess of Calculated Lower Bound	18
Figure 4:	Sea Surface Backscatter Strength as a Function of Beam Width and Water Depth	19
Figure 5:	EDO-65 Transducer	20
Figure 6:	Parametric Source Level	21
Figure 7:	Parametric Beam Width	22
Figure 8:	Pulsed CW Operation	23
Figure 9:	Correlation Operation	24
Figure 10:	Conventional Beam Pattern at 13.4 khz	25
Figure 11:	Parametric Beam Pattern at 13.4 khz	26
Figure 12:	Conventional Beam Pattern at 68 khz	27
Figure 13:	Reduced Power Parametric Beam Pattern at 13.4 khz	28
Figure 14:	Conventional Beam Pattern at 19.3 kHz	29
Figure 15:	Parametric Beam Pattern at 19.3 kHz	30
Figure 16:	Pulsed CW Scan with a 6 Second Range	31
Figure 17:	Pulsed CW Scan with a 10 Second Range	32
Figure 18:	Effect of Elevation Angle, 2.0° Down to Horizontal	33
Figure 19:	Effect of Elevation Angle, 1.0° Up to 2.5° Up	34
Figure 20:	Ray Trace for Beam Directed 2.0° Below Horizon	35
Figure 21:	Ray Trace for Beam Directed 1.0° Below Horizon	36
Figure 22:	Ray Trace for Horizontal Beam	37
Figure 23:	Ray Trace for Beam Directed 0.5° Above Horizon	38

Figure 24:	Ray Trace for Beam Directed $1.0^\circ$ Above Horizon	39
Figure 25:	Ray Trace for Beam Directed $2.0^\circ$ Above Horizon	40
Figure 26:	Results of Correlation Operation	41
Figure 27:	Ray Trace for Makassar Strait, Positive Gradient, 10 Meter Source Depth	42
Figure 28:	Ray Trace for Makassar Strait, Positive Gradient, 20 Meter Source Depth	43
Figure 29:	Ray Trace for Makassar Strait, Positive Gradient, 30 Meter Source Depth	44
Figure 30:	Ray Trace for Makassar Strait, Positive Gradient, 40 Meter Source Depth	45
Figure 31:	Ray Trace for Makassar Strait, Negative Gradient, 10 Meter Source Depth	46
Figure 32:	Ray Trace for Makassar Strait, Negative Gradient, 20 Meter Source Depth	47
Figure 33:	Ray Trace for Makassar Strait, Negative Gradient, 30 Meter Source Depth	48
Figure 34:	Ray Trace for Makassar Strait, Negative Gradient, 40 Meter Source Depth	49



## I. INTRODUCTION

The Navigation Hazard Survey Sonar is a side-looking sonar with a range of 2 nautical miles (nm). Its purpose is to sweep a 4 nm swath between tracks of a survey ship in order to detect surface and submarine navigation hazards in straits, passes, sea lanes, and coastal waters.

The sonar will be used as a decision tool during the actual conduct of a hydrographic survey. A wide track spacing may be maintained as long as no navigation hazards are detected. When a hazard is detected, the survey ship can either deviate from its course for detailed survey of the detected hazard or alternate survey assets can be deployed.

The basic contribution of the subject sonar to a hydrographic survey effort is the confidence -- backed up by hard-copy sonar imagery -- that no unknown navigation hazards exist in the space between widely spaced ship's tracks. The wide track spacing made possible by this confidence will permit limited ship resources to be used more efficiently by reducing the time spent surveying a given area. In addition, it will contribute to the safety of survey ships operating in unknown areas.

### A. BACKGROUND

A concept design study (Fagot, 1978) was performed for the Defense Mapping Agency to define a side-looking reconnaissance sonar with an athwartship range of 16.7 kilometers (km) (9 nm) to detect topographic features in the deep ocean that are hazards to submarine navigation. This study identified a candidate system (AN/SQS-56) with performance projected to meet the desired range capability, but the system's large physical size limits its application in coastal waters where smaller survey craft are employed.

The SEASAT system is potentially capable of remotely detecting large navigation hazards with a substantially greater coverage rate. However, water depth in excess of 2700 meters (m) is required for reliable detection of seamounts without excessive false alarms.

A gap exists in the Navy's technology to rapidly survey wide swaths (4 to 6 nm) in water depths less than 2700 m for navigation hazard detection. A navigation hazard survey sonar is required to close this gap and eliminate the need for expensive, close-track surveys with conventional depth sounders. Such a sonar must be smaller, lighter, less expensive, and less sensitive to refraction than the long-range reconnaissance sonar. To be fully responsive to the requirement, it should be air transportable. In addition, it must have improved performance capability over existing or newly emerging side-looking type sonar systems.

The major technical risk is the development of system acoustic and geometrical characteristics to permit insonification of features at long athwartship ranges, in the presence of refraction and the relative proximity of ocean boundaries (surface and bottom) in coastal waters, and in the development of the necessary acoustic and signal processing techniques to minimize detection of false targets.

The ability to insonify features at long athwartship ranges that extend into depths that constitute a hazard is controlled by refraction. This was certainly the case for the deep water, long range, reconnaissance sonar (Fagot, 1978). In shallow water the sound velocity structure can be irregular and greatly influenced by surface heating and cooling, salinity changes, and water currents. Improvements in

the sonar's ability to insonify hazards can be achieved by placing the array at a depth of more optimum sound velocity conditions. This can be obtained by employing a towed array, thus operating in a variable depth sonar (VDS) configuration.

Hazards are distinguished from false targets on the basis of minimum measured depth. The precision of this process is limited by shadow zones which obscure hazard summits and by beamwidth. Shadow zones can be extended by range by employing the VDS configuration noted.

The hazard-type sonar is only interested in detecting minimum depths within its survey range. A wide beamwidth system will not only detect minimum target depths, but will also insonify and detect deeper false targets, whereas a narrow-beam system will reduce false target detection. Achieving a sufficiently narrow beam while keeping transducer array size compatible with a portable unit requires careful tradeoffs between array size, frequency, and source level, based on anticipated environmental conditions.

#### B. ALTERNATE APPROACHES

The General Instrument Corporation, Harris ASW Division, produces a swath contouring system, designated the Bathymetric Swath Survey System (BS<sup>3</sup>). This system produces real-time contouring charts of shoaling trends. The system employs 21 performed 5° beams for a maximum athwartship span of + 52.5° from the vertical. The span width employed in generating the contour chart is a function of the ship's roll and noise. In high roll and noise condition, the questionable data from the outermost beam is not used in generating the contour chart; however, the total span is never less than + 27.5° (11 beams). The maximum athwartship range on each side of the survey vessel is limited to 1.3 times the water depth. For example, a range of 910 m could be achieved in water depths of 700 m for a flat bottom. Although accurate depth contours can be obtained with this system, the range capability does not meet the required hazard survey sonar objective.

Another approach to hazard detection is to employ a conventional side-scan sonar. The model 606 manufactured by EDO Western Corporation is typical of this class of sonar systems. In addition to the side-scan capability, these systems can also include a bathymetry or subbottom profiling-option.

Side-scan sonars produce displays of port and starboard bottom features somewhat similar to a continuous high altitude aerial photograph. The features appear as highlights and shadow zones. The heights of the features are implied from the length of the shadow zones considering the geometry imposed by the operational configuration. The interpretation of side-scan records is somewhat judgmental even for the trained observer. This point is discussed in a comprehensive theoretical and practical review of the side-scan sonar techniques presented by Leenhardt (1974) and Fleming (1976).

Side-scan sonars have high resolution, both angular (narrow horizontal beamwidth) and range (short pulse length), but are limited to short range due to their high operating frequency. The Kelvin Hughes system operates at a lower frequency than the EDO system, near 36 kHz, and has a range capability varying between 1000 and 1500 m.

The prime factors limiting use of off-the-shelf side-scan sonars as described above for the long-range hazard sonar application is the short-range limitation, the display interpretation difficulty, and the proximity of the water surface in coastal waters.

The British Department of Industry is developing a sector scanning sonar, Hydrossearch, designed for hydrographic sea-bed surveying (Colvin, 1976).

The model can be operated in two modes. The horizontal mode allows azimuth scanning in a forward-looking direction. For this mode, the scanning sector is wide in the athwartship direction. The vertical mode allows depth scanning in a side-looking direction. For this case, the scanning sector is wide in depth direction.

The Hydrossearch system employs a scanning technique known as modulation scanning. This technique allows rapid scanning of a broad sector (30° or 60° sector) containing many preformed beams, each controlled in width by the aperture (array size) and operating frequency. Narrow beams can be obtained with large arrays of high-operating frequencies. For example, the Hydrossearch Model A can scan a 60° sector with a 0.5° angular resolution, but requires an operating frequency of 180 kHz and a 1 m array length.

Although this system allows high angular resolution, and thus, precise feature height determination in the vertical mode, the system's high operating frequency precludes the long-range capability desired for hazard detection sonar.

## II. BEAM PATTERN CONSIDERATIONS

Conventional side-scan sonars utilize fan-shaped acoustic beams. These beams are narrow in the fore-aft direction, and broad in the depth-elevation direction. These conventional sonars are normally towed sufficiently deep to avoid ambiguous reflections from the water surface. The Navigation Hazard Survey Sonar, on the other hand, cannot be towed as deep because its range substantially exceeds the depth of the coastal waters in which it must operate. Therefore, if the water surface is rough enough to be a good scatterer, any sound which strikes the surface at large grazing angles will create ambiguous imagery which will be difficult to distinguish from actual topography. This problem can occur whether the sound reaches the water surface directly, or by the bottom-reflected path. Therefore, for coastal surveying in moderate or high seas, the transmitted sound and/or receiver sensitivity must be confined vertically to within a narrow beam. Since the beam pattern must also be narrow in the fore-aft direction for good along-track resolution, a conical beam is indicated. Side-lobes must be kept as low as possible to avoid unwanted side-lobe reflections from the water surface.

To obtain a lower bound on the required beamwidth, it is convenient to assume that the beam must be sufficiently narrow to prevent the insonification of the water surface, either by the direct or bottom-reflected path. The results so obtained can be increased slightly through a more detailed consideration of the variation of sea surface backscatter strength with grazing angle, frequency, and wave height.

Figure 1 shows a side-scan sonar operating in shallow, constant depth, isovelocity water. The beamwidth  $\theta$  is assumed to be narrow. The elevation angle is adjusted so that the direct and bottom-reflected beam-edge rays strike the water surface at the same horizontal range. The required beamwidth is given by:

$$\theta = \tan^{-1} \left( \frac{2 D_w - D_f}{R} \right) + \tan^{-1} (D_f/R) \quad (1)$$

where  $D_w$  is the water depth,  $D_f$  is the depth at which the sonar is towed, and  $R$  is the limiting horizontal range. If the small angle approximation is made, this reduces to:

$$\theta = \tan^{-1} (2 D_w/R) \quad (2)$$

Figure 2 gives the lower bound on required beamwidth, as calculated from equation (2), for ranges of 1850 m (1 nm) and 3700 m (2 nm).

Schulkin and Shaffer (1964) developed the following empirical equation for sea surface backscatter:

$$N_{ss} = 9.9 \log (f h \sin \beta) - 45.3 \quad (3)$$

where  $N_{ss}$  is the sea surface backscatter strength in decibels (dB),  $f$  is the frequency in kHz,  $h$  is the peak-to-trough wave height in feet, and  $\beta$  is the grazing angle. Referring to Figure 1, if the beamwidth is increased to  $\theta + \Delta\theta$ , and the excess beamwidth is taken toward the water surface as shown, the grazing angle for the upper beam-edge ray is given by

$$\beta = \tan^{-1} (D_f/R) + \Delta\theta \quad (4)$$

Figure 3, which is based on equations (3) and (4), gives the sea surface backscatter strength resulting from beamwidths in excess of those specified by Figure 2, assuming a 30 m tow depth, a 3700 m range, and a frequency of 13 kHz. Note that a  $1.0^\circ$  excess beamwidth in 10 foot (ft) seas will produce a sea surface backscatter strength of about -40 dB/m, which is a level typical of a poorly reflecting ocean bottom. If we wish to keep sea surface backscatter strengths lower than 9 or 10 dB below the backscatter strength of such a bottom, we can only exceed the beamwidth criteria of Figure 2 in very calm weather. For rocky bottoms with backscatter strengths on the order of -15 to -20 dB/m<sup>2</sup>, the beamwidth criteria of Figure 2 can be exceeded by several degrees.

Figure 4 shows the expected sea surface backscatter strengths for various water depths and beamwidths, assuming 5 ft waves, 3700 m range, 30 m tow depth, and 13 kHz operation. For depths deeper than those plotted, sea surface reverberation will occur outside the range of the sonar, and therefore will not affect system operation. When sea surface reverberation does occur within sonar range under the stated conditions, it will not interfere with reverberation from rocky bottoms which have much higher backscatter strengths (on the order of -20 dB/m<sup>2</sup>). Sea surface reverberation will be only marginally distinguishable from low reflectivity flat mud bottoms (backscatter strength about -40 dB/m<sup>2</sup>). Therefore, the conservative design approach is to use a beamwidth which keeps the sea surface reverberation outside the sonar range. Thus, a  $1.5^\circ$  beam is indicated for a minimum mid-range depth of 50 m; a  $2^\circ$  beam is indicated for a minimum mid-range depth of 65 m, a  $2.5^\circ$  beam is indicated for a minimum mid-range depth of 80 m, and so forth. However, Figure 2 indicates that these beamwidths will permit operation in water depths of 25, 35, and 50 m, respectively, at a range of 1850 m.

The previous discussion must be applied cautiously because of the isovelocity, constant depth assumptions. Larger beamwidths (or shallower depths) can be used when sounding upslope. When oceanographic conditions permit surface duct propagation, extended ranges can be achieved in shallow water by intentionally bouncing sound off the water surface. However, refraction normally increases the water depths required to achieve a given range with a given vertical beamwidth. Also, the fit of empirical data to equation (3), as reported by Schulkin and Shaffer (1964), involves a standard deviation of 5.4 dB.

Forming beams in the  $1.5^\circ$  to  $2.5^\circ$  range, at a frequency low enough to permit a 3700 m range, would be straightforward if we had the luxury of specifying a transducer 2 to 3 m in diameter. The handling problems and cost associated with such a transducer would be prohibitive. On the other hand, restricting the active diameter of the transducer to about 0.51 m (20 in) would lead to a relatively easy-to-handle towed body. The following calculation illustrates the difficulty associated with attempting to utilize conventional beamforming techniques under such a size restriction.

Forming a  $2.5^\circ$  beam with a 0.51 m diameter transducer requires an operating frequency of 70 kHz. Such a projector would have a directivity index of 37.4 dB. Allowing 0.3 watts per square centimeter of projector area, a source level of 237 dB/ $\mu$ Pa/m could be achieved. The reverberation level resulting from targets on the ocean floor is given by

$$RL = SL - 40 \log R - 2 \alpha R + TS \quad (5)$$

where RL is the reverberation level (the desired signal), R is the range,  $\alpha$  is the absorption in dB/m, and TS is the target strength of the bottom or any object of interest on the bottom. Using  $R = 3700$  m and  $\alpha = 0.018$  dB/m, this becomes

$$RL = TS - 39 \quad (6)$$

The minimum reverberation level which can be received is given by

$$RL \geq NS + 10 \log W - DIR + DT \quad (7)$$

where NS is the noise spectral density, W is the receiver bandwidth, DIR is the receiver directivity index, and DT is the detection threshold. Assuming sea state 3 and neglecting flow noise and own-ship radiated noise,  $NS = 33$  dB/ $\mu$ Pa/Hz. Assuming a 10 millisecond tone burst transmission (for 7.5 m range resolution), a receiver bandwidth of 100 Hz would be required. Using 10 dB for DT and 37.4 dB for DIR, equations (6) and (7) reduce to

$$TS \geq 64.4 \text{ dB}$$

which is an impossible requirement. A large target, such as a beam aspect submarine, has a target strength the order of 25 dB.

The absorption term  $2 \alpha R$  was 133 dB in the preceding calculation. This high absorption makes it impossible to balance the sonar equation at 70 kHz. Therefore, it is necessary to utilize nonlinear acoustics technology to form the required narrow beam at lower frequency.

### III. NONLINEAR ACOUSTICS

Nonlinear acoustics techniques involve insonification of a volume of sea water at very high intensities, such that the difference in sound speed between the peaks and troughs of the sound waves (resulting from the variation of sound speed with pressure) is significant. Under these conditions, peaks will travel faster than, and eventually overtake, the troughs of the acoustic waves. In this manner, a transmitted sine wave will be transformed to a sawtooth wave. At greater ranges, selective absorption of the high frequency content of the sawtooth wave will "round off the corners" of the sawtooth wave, causing it to degrade again into a sine wave. Nonlinear phenomena take place in the volume of water bounded near the transducer by the range at which the peaks overtake the troughs, away from the transducer by attenuation, and axially by the projector beam pattern. If two high-intensity sine waves are transmitted, sum and difference frequencies are generated in the aforementioned volume of water, which acts like a very large, although less powerful, end-fired projector array. The sum and difference frequencies have approximately the same beam pattern as the primary frequencies, except that the main lobes are slightly wider and the side lobes are substantially reduced. Frequency-selective absorption favors the difference frequency; at large ranges the difference frequency is normally the only significant radiation.

Up to a point, the efficiency of this process increases with source level. At very high source levels, however, the region of nonlinear interactions broadens, resulting in a broadening of the secondary frequency beamwidth and a reduction of the efficiency of the process.

### IV. SOURCE PERFORMANCE PREDICTION

#### A. SOURCE LEVEL

The model developed by Moffet and Mellen (1977) was utilized to calculate the source level of nonlinear, or parametric projectors. More specifically, design curves based on this model were obtained from the authors, and applicable portions of the curves were tabulated in a computer-compatible form. A program to perform tabular lookup, interpolation, and all calculations associated with the use of these design curves was written for the Hewlett-Packard Model 9845 calculator. The required inputs are primary frequency, primary frequency source level, secondary frequency, projector diameter, and the absorption coefficient at the primary frequency. The results are valid in the far field for circular and square piston projectors. Near-field measurements will normally be lower than the calculated results, by an amount which can be determined through reference to the curves in Mellon's report on a near-field model (1976). Any distance greater than  $100 \alpha A/\lambda$ , where  $\alpha$  is the absorption coefficient,  $A$  is the projector area, and  $\lambda$  is the primary frequency wavelength, may be considered far field. However, source levels often do not decrease by more than a few decibels until the distance is reduced to a substantially lower value. Also, the reduction of source level with decreasing range is substantially less than the opposing reduction of spherical spreading loss; systems with adequate source level in the far field will have adequate source level well into the near field.

## B. BEAMWIDTH

The model developed by Moffet and Mellon (1977) was used to calculate the beamwidths of nonlinear acoustic projectors. Design curves obtained from the authors were computerized as in the source level model. Rigid piston theory was used to convert the secondary frequency directivity index obtained from the Moffet/Mellon curves to a 3 dB beamwidth.

Observation of beam patterns in the near field will tend to make the apparent beam patterns broader than the more operationally significant far-field patterns. This near-field beamwidth broadening occurs under the same conditions that produce a near-field source level reduction. Thus, the less intense near-field beam occupies more space, thereby conserving total energy.

Measured far-field parametric beamwidths are frequently smaller than those predicted by the above technique by as much as 30%, due to a number of approximations made by Moffet and Mellon (1977) in order to present the theoretical results in the convenient design curve form. These approximations are discussed in their paper, which also presents a direct integration calculation technique that is more accurate, but which requires substantial amounts of computer time.

If beamwidths must be known closer than  $\pm 30\%$ , it is necessary to calibrate the computerized design curve calculations with the more elaborate numerical integration technique, or with experimental data.

## C. SOURCE DESCRIPTION

The source shown in Figure 5 has an overall diameter of 1 m and an acoustic aperture of 0.9 m. The source level at 13.4 kHz and 19.3 kHz is shown in Figure 6, based on a primary frequency of 68 kHz. The absorption coefficient used was 0.0019 dB/m, which is appropriate for the 39°F, fresh-water conditions encountered during the feasibility demonstration experiment. The data points were measured at a projector-to-hydrophone distance of 42.5 m, and were corrected to farfield using Mellon's curves (Mellon, 1976). The near-field correction was 7.2 to 9.0 dB at the lower sound levels and 0.2 to 1.7 dB at the higher sound levels. The close agreement between theory and experimental data indicates that the source level model can be used with confidence in the design of the system.

The secondary frequency beamwidth is given in Figure 7. The data agree well with the theory at high source levels, but there is a 0.2 to 0.3° discrepancy in the 231-236 dB/ $\mu$ Pa/m range. The direction of this discrepancy is consistent with the hypothesis that it is due to the near-field measurement.

## V. FEASIBILITY DEMONSTRATION EXPERIMENT

A feasibility demonstration experiment was performed with the Naval Underwater Systems Center at their Seneca Lake Sonar Test Facility during April 1979. The Transducer Calibration Platform (TCP), which is moored in 153 m of water, was utilized. This experiment involved the use of azimuthal transducer rotation to collect side-scan sonar imagery, since an appropriate tow vehicle was not available. The water was isothermal at 39°F.

### A. APPARATUS

The projector shown in Figure 5 was mounted on the end of a 33 m shaft in a manner which permitted the projector to be turned in both azimuth and elevation.

A pendulum potentiometer was used to sense the elevation angle. Several hydrophones were deployed at depths of 34-36 m at a range of 42.5 m for the measurement of beam patterns.

### 1. Pulsed CW Operation

Figure 8 shows the electronic setup for pulsed CW operation. The frequencies and filter settings shown are for 19.3 kHz operation with a 10 ms pulse.

The apparatus utilizes a modulator which accepts as inputs, tones at both the desired primary frequency and half the desired secondary frequency. The output consists of two frequencies centered around the desired primary frequency and separated by the desired secondary frequency. In Figure 8, inputs at 68 kHz and 9.65 kHz result in frequencies of 58.35 kHz and 77.65 kHz being applied to the input of the power amplifier.

The operating cycle is initiated by a key pulse from the line-scan recorder. In response to this keypulse, a synchronizer first switches the T/R switch to the transmit position, and then applies a gating pulse of controlled duration (10 ms) to the power amplifier, enabling it to pass and amplify the signal. The T/R switch passes the signal to the transducer.

Nonlinear acoustic phenomena in the water cause the difference frequency of 19.3 kHz to be generated. This signal propagates to the target and returns to the transducer. By this time the T/R switch has returned to the receive position, and the signal is amplified and filtered to a bandwidth of approximately 1 kHz. A beat frequency oscillator (BFO) set to 20 kHz beats the 19.3 kHz down to 700 Hz in a second modulator, and the filter F3 limits the bandwidth to the reciprocal of the pulse length. The illustrated 650 to 750 Hz bandwidth is appropriate for a 10 ms pulse length.

Operation at other frequencies involves changing the lower frequency input to the transmitter's modulator to half the desired secondary frequency, centering filters F<sub>1</sub> and F<sub>2</sub> around the new frequency, and changing the BFO frequency or the center frequency of filter F3 to assure that the down-shifted frequency is in the center of the filter passband.

### 2. Correlation Operation

Figure 9 shows the electronic setup for correlation operation. Operation at 13.4 kHz is illustrated. The operating cycle is initiated by a key pulse from the line-scan recorder. In response, the synchronizer sequentially switches the T/R switch to the transmit position, enables the power amplifier, and keys the correlator. The correlator then outputs on FM slide waveform centered around 3.5 kHz. The waveform has a bandwidth of 2 kHz, thus occupying the spectrum from 2.5 kHz to 4.5 kHz. The correlator retains in memory (the memory in the case of the CESP-II is hard-wired) a detailed replica of the FM slide waveform.

A 9.9 kHz tone is used to beat the FM slide waveform up to a center frequency of 13.4 kHz, the desired secondary frequency. A filter set to a passband of 10 to 20 kHz eliminates the modulation harmonics.

A second modulator adds a 61.3 kHz carrier. The result is an FM slide centered on 74.7 kHz plus a 61.3 kHz tone. This signal is amplified and passed to the transducer.



Nonlinear acoustic phenomena in the water cause the difference frequency signal, consisting of an FM slide centered at 13.4 kHz, to be generated. This signal propagates to the target and returns to the transducer. By this time the T/R switch has returned to the receive position. The signal is then amplified and filtered to a bandwidth of 6 kHz. The bandwidth is purposely kept large at this point to minimize phase distortion.

The received signal is then beat back to the 3.5 kHz range by the same 9.9 kHz signal that was originally used to beat the transmit signal up to 13.4 kHz. The resulting 3.5 kHz FM slide is coherent with the replica of the transmitted waveform which is stored in the correlator's memory.

The correlator compares the recent history of the received signal with the stored replica; and outputs to the line-scan recorder a signal proportionate to the (hard-clipped) cross correlation product, which is a measure of similarity of the two signals. This process is described in greater detail by Moss and Walsh (1970).

By utilizing all of the energy in a long pulse for detection, the correlator produces a signal processing gain equal to the increased energy relative to a CW pulse with the same (2 kHz) bandwidth. For a 100 millisecond pulse this amounts to 23 dB.

The range resolution is equal to the reciprocal of the bandwidth, which is 0.5 ms, or 0.375 m. The signal processing gain is needed to compensate for the relatively small ocean floor area contributing to the received signal in any single resolution cell.

#### B. EDGE-ON FREQUENCY RESPONSE

In a towed sonar it is desirable to minimize the sensitivity of the transducer to noise radiated by the towing vessel, assuming that the noise field is not dominated by flow noise. For an athwartship-oriented beam, this means that the side lobes toward the edge of the transducer should be kept at a minimum.

In order to determine the frequencies which would produce the minimum edge-on sidelobes with the ED0-65 transducer, the transducer was oriented 90° away from the test hydrophone and the transmitted source level was measured as a function of frequency. The transmit rather than the receive response was measured for reason of experimental convenience, but both have similar (linear acoustics) beam patterns because of reciprocity. Nulls were noted at 13.4 kHz, 17.2 kHz, and 19.3 kHz. The two extreme frequencies were then selected for further testing.

#### C. BEAM PATTERNS

Figure 10 shows the beam pattern when the transducer is excited in the conventional (linear acoustics) manner at 13.4 kHz. Nonlinear excitation of the same transducer, with a primary frequency of 68 kHz and a secondary frequency of 13.4 kHz, results in the substantially narrower beam pattern of Figure 11. The only discernible side lobe is 47 dB down from the major response axis. This small side lobe results from an anomaly in the primary frequency beam pattern (Fig. 12). Even this small side lobe can be reduced below the 0 to -50 dB range of the beam pattern measurement instrumentation by reducing the power applied to the transducer, as shown in Figure 13.

Figures 14 and 15 show the conventional and parametric beam patterns of the same array at 19.3 kHz. The anomalous side lobe in this case is somewhat stronger.

The substantial reductions in beamwidth and side lobe levels make nonlinear acoustics an effective tool for probing between the water surface and the bottom at long ranges in coastal waters when searching for navigation hazards.

#### D. PULSED CW OPERATION

For azimuthal scans of the lake, the reference bearing was defined as the bearing to the test hydrophones. This reference was chosen so that the hydrophone could be used to reset the bearing indicator in the event of loss-of-reference. Thus, the reference bearing was approximately north-northwest. With this reference bearing, the Systems Measurement Platform (SMP) could be detected acoustically at a bearing of 338°.

The transducer was rotated clockwise at a rate of one revolution per hour, and pulsed for 10 ms at 19.3 kHz every 6 seconds (sec). The elevation was 0.3° above the horizon. The primary frequency source level was 243.5 dB// $\mu$ Pa//m. According to Figure 3, the far-field secondary frequency source level was 224 dB// $\mu$ Pa//m. The received signal, processed as in Figure 8, was applied to the line-scan recorder. The resulting image is shown in Figure 16.

The full range of 6 seconds is equivalent to 2.3 nm. Time increases from the bottom to the top of Figure 16.

The scan starts at a relative bearing of 300°, showing the west shore of Seneca Lake, including some near-shore topography. As the transducer swings around to 330°, a ridge shows up clearly at maximum range. Immediately thereafter, a series of six reflections associated with the two hulls and four-point mooring system of the SMP appears at a relative bearing of 339° and a range of 2.2 nm. The beam then traverses open water near the northwest, finally picking up the east shore at a relative bearing of 0°. The eastern shore has its closest approach around 60°. Several interesting bottom features show up along the southern extreme of the eastern shore, and near relative bearing 180°, during which time the beam is insonifying the open water to the south. The western shore of the lake comes in again for relative bearings of 200-330°. A number of fish are evident at close ranges for all bearings.

The receiver gains were set so that echoes could be received at full range. As a result the very strong reflections from shorelines at ranges of only approximately 0.5 nm saturated the recorder, causing loss of detail. This problem could be remedied by a time-varied gain circuit.

Another scan of the lake is shown in Figure 17. In this case the pulse repetition rate was 10 sec, corresponding to a maximum range of 3.8 nm in fresh water. The elevation angle was 1.0° above the horizon, and the operating frequency was 13.4 kHz. The primary frequency source level was 247 dB// $\mu$ Pa//m. According to Figure 3, the corresponding secondary frequency source level is 221 dB// $\mu$ Pa//m. Comparison with Figure 16 indicates that some features show up more distinctly, others less.

The 270-360° sector was scanned repeatedly at 19.3 kHz, using 10 ms pulses at a variety of elevation angles. The results are shown in Figures 18 and

19. Significant differences between images result from differences in elevation angle as small as  $0.5^\circ$ . This indicates that the beam in a practical towed system must be roll stabilized. It also suggests the possibility that data collected at various elevation angles can be used to quantify some of the topographic details, assuming that insight gained from a more detailed study of the physics of this phenomenon can be used to design the appropriate displays.

A second observation from Figures 18 and 19 is that longer ranges seem to be attainable with the transducer pointed above the horizon. In an attempt to explain this trend, a sound speed cast was taken and ray traces were computed for a  $2.0^\circ$  beam directed in a variety of elevation angles. The results are shown in Figures 20 through 25. It can be seen that at a range of 4000 m, for example, the upward-directed rays intercept the bottom at steeper angles than the downward-directed rays, and therefore encounter greater bottom backscatter strengths. It is significant that Figure 19 shows no evidence of interference from water-surface reverberation. Thus, reflection from the water surface enhanced rather than degraded the system performance. However, Figure 3 indicates that the lack of sea surface backscatter interference cannot be relied upon in the open ocean in high sea states.

Scanning was attempted with both 1 ms and 100 ms CW pulses. The 1 ms pulse did not produce enough signal-to-noise to form a good image. The 100 ms pulse produced an intense image, but the smearing in time seriously degraded the quality of the image.

Another experiment indicated that the primary frequency source level could be reduced by 12 dB without loss of signal, but not by 18 dB, when a 10 ms CW pulse was used. With a 100 ms CW pulse, the primary frequency source level could be reduced by 18 dB without loss of signal. Reduction of the source level substantially reduced the dynamic range of the imagery.

#### E. CORRELATION OPERATION

Correlation operation, using the apparatus of Figure 9, is depicted in Figure 26. The beam was directed  $1.0^\circ$  above the horizon. A 100 ms FM slide waveform with a 2 kHz bandwidth centered about 13.4 kHz was used. The source level was 247 dB/ $\mu$ Pa/m at the primary frequency, and 221 dB/ $\mu$ Pa/m at the secondary frequency. The repetition rate was 10 sec.

Sand steps can be seen on the slopes rising to the eastern and western shores of the lake. Notice the six echoes from the SMP in a local white background near top center (half-range, at a bearing of  $340^\circ$ ). Examination of the second of these echoes, using the original data rather than the photographic reproduction in this report, indicates a double structure, as if sound reflected from both the front and the back of some object were separately resolvable.

Comparison of Figure 26 with Figure 17 indicates that large features such as shorelines, points, and underwater ridges show up best with CW pulses, and that such small features as sand steps and manmade objects show best with correlation.

## F. SUMMARY OF EXPERIMENTAL RESULTS

The following experimental results were obtained:

1. Imagery could be obtained to a range of 3.8 nm under the conditions encountered.
2. Large features such as shorelines, points, and underwater ridges appeared best with CW pulses of at least 10 ms.
3. Small features such as sand steps and manmade objects appeared best with correlation.
4. Six separate echoes were obtained from a catamaran barge (the SMP) with a four-point moor, located at a range of 2 nm. With correlation, one of these echoes showed structure, suggesting separate reflections from the front and back of some object.
5. Several interesting echoes, suggesting objects on the lake bottom, were noted.
6. Results were very sensitive to elevation angle, with changes as small as  $0.5^\circ$  causing a noticeable difference. This indicates a requirement for beam steering in the vertical direction to correct for vehicle roll.
7. Best results were obtained with the beam tilted slightly above the horizontal. Under these conditions, the sound was bounced off the water surface. This resulted in larger grazing angles and a higher bottom backscatter strength.

## VI. REFRACTION

Refraction effects were considered for the Makassar Strait, an area where the Naval Oceanographic Office has extensive survey commitments. A computer search turned up two typical sound speed profiles within the area bounded by  $0^\circ 0'N$ ,  $1^\circ 40'S$ ,  $116^\circ 30'E$ , and  $119^\circ 38'E$ . The two profiles were similar, except that one had a slightly positive sound speed gradient in the mixed layer, while the other had a slightly negative gradient.

Figures 27 through 30 show the coverage patterns for horizontally directed  $2^\circ$  beams towed at 10, 20, 30, and 40 m, respectively, for a sound speed profile with a slightly positive gradient in the mixed layer. At a tow depth of 10 m, a range of 4000 m appears achievable in water as shallow as 30 m, provided that the sea surface conditions can support the surface duct mode of propagation.

As the source is lowered to 30 m, the energy becomes split between two different paths, as shown in Figure 29. This effect would complicate data interpretation. The energy splitting effect disappears as the source is lowered to a depth of 40 m, as can be seen Figure 30. At this depth the energy is confined to the downward refracted path. Refraction would then limit the range approximately 2200 m for a water depth of 150 m, although greater ranges could be achieved in deeper water.

Figures 31 through 34 show the coverage patterns under the same conditions, except that the sound speed profile has a slight negative gradient in the mixed layer. The energy is confined to the downward refracted path in all cases. The

refraction-limited range is greatest at shallow tow depths, but the sound is more tightly focused and would produce a higher signal-to-noise ratio at a tow depth of 40 m. A range of 1900 appears feasible for a water depth of 150 m and a tow depth of 40 m.

Comparison of Figure 27 with Figure 31 reveals a profound change in system performance, resulting from a subtle difference in the sound speed profile. It follows that taking advantage of the higher potential ranges of the 10 m tow depth would require an astute awareness of small changes in the sound speed profile on the part of the survey party. By contrast, a comparison of Figure 30 with Figure 34 indicates relatively stable performance for a 40 m tow depth.

For either sound speed profile considered, a range of 4000 m appears feasible in water depths of 650 m or more.

## VII. SUMMARY AND RECOMMENDATIONS

When attempting to use a side-scan sonar with a 2 nm range in coastal waters, the relative proximity of the ocean surface and bottom relative to the range becomes an important consideration. If the sea is not unusually calm, narrow vertical beamwidths must be used to avoid ambiguous backscatter from the ocean surface. This contrasts to conventional side-scan sonars which utilize fan-shaped beams that are broad in the vertical direction.

The requirements for vertical beamwidths were quantified for the special case of isovelocity water and constant water depth. Assuming that the sea state is so high that acoustic encounter with the surface must be avoided, beamwidths of 1.5-2.5° are indicated for water depths of 50-80 m at a 3700 m horizontal range, or for water depths of 25-50 m at an 1850 m horizontal range. However, these beamwidths can be exceeded by several degrees for low wave height, a strong reflecting bottom, or deeper water depths.

A consideration of the design tradeoffs related to transducer size, frequency, absorption, and beamwidth led to the conclusion that conventional linear acoustic techniques could not be used, given the constraint that a transducer aperture the order of 0.5 m was desirable for convenience in handling and towing.

Nonlinear acoustics were discussed as an approach to the formation of narrow beams at frequencies low enough to propagate the required distance. Methods to calculate the source levels and beamwidths of parametric beams were discussed, and the results of sample calculations were presented. Experimental data verified that the source level calculation techniques were within 2 dB/ $\mu$ Pa/m.

A feasibility demonstration experiment utilizing available equipment was performed at the Naval Underwater Systems Center Seneca Lake Sonar Test Facility during April 1979. During this experiment, a transducer with a 0.9 m aperture was rotated in azimuth and excited parametrically. Side-scan sonar imagery could be obtained to a range of 3.8 nm. Large features such as shorelines, points, and underwater ridges showed up best with 10 ms CW pulses. Small features such as sand steps and manmade objects showed up best with replica correlation signal processing. The test results were very encouraging. However, the tests were performed in a benign lake environment from a stable platform. System performance in an environment which includes flow noise, vehicle motions, and moderate seas has yet to be determined.

The effect of refraction was explored for a specific area within the Makassar Strait. It was found that towing a horizontally oriented projector at a depth of 40 m would result in ranges from 1900 m in 150 m deep water to 4000 m in 650 m deep water. Towing at shallower depths would produce longer ranges in shallower water some of the time, but the actual results would be highly sensitive to environmental conditions. As an extreme, a range of 4000 m could be achieved in water as shallow as 30 m, assuming a slightly positive sound speed gradient in the mixed layer and very calm seas. Shallow towing, however, requires the survey party to keep on top of small changes in the sound speed profile.

The next step, if additional work can be performed, is to build a tow vehicle and a mechanism to stabilize the beam against vehicle roll. The most suitable existing transducer for such an experiment is the SPA transducer, which has a physical diameter of 0.6 m and an acoustic aperture of 0.51 m. The primary frequency is 60 kHz, and the achievable range of secondary frequencies has yet to be determined. For a 214 dB/ $\mu$ Pa/m secondary frequency source level, the anticipated beamwidth is 2.4° to 3.2°, depending on the secondary frequency. The SPA transducer is compatible with electronic beam steering in one direction, by virtue of its division into staves. An appropriate tow vehicle could be constructed based on an adaptation of the XU-1245 variable-depth-transducer housing (Brisbane, 1962), which has an overall length of 1.3 m, and accommodates a 0.46 m diameter cylindrical transducer in a side-looking orientation.

#### VIII. REFERENCES

- Brisbane, Arthur P. (1962). Hydrodynamic Characteristics of the XU-1245 Variable-Depth-Transducer Housing. David Taylor Model Basin Report 1654.
- Buckley, J. P. and R. M. Urick (1968). Backscattering from the Deep Sea Bed at Small Grazing Angles. J. Acous. Soc. Am., v. 44, n. 2, p. 648-654.
- Colvin, D. W. (1976). An Advanced Sonar for Hydrographic Survey. Presented at the Eighth Annual Offshore Technology Conference, Houston, Texas, OTC Paper Number 2658, May.
- EDO Western Corporation. Model 606 Side-Scan Sonar System. EDO Western Corporation, Salt Lake City, Utah, manufacturer brochure.
- Fagot, M. (1978). Reconnaissance Sonar Concept Design Study -- Final Report. Naval Ocean Research and Development Activity, NSTL Station, Miss., NORDA Technical Note 17.
- Flemming, B.W. (1976). Side Scan Sonar: A Practical Guide. Int. Hydrog. Rev., 53(1), p. 65-92.
- Harris, ASW Division. BS<sup>3</sup> Bathymetric Swath Survey System -- A Computer Processed Multibeam Sonar for Precise Bathymetric Survey. General Instruments Corporation, Harris Division, Westwood, Mass., 02090, manufacturer brochure.
- Leenhardt, O. (1975). Side Scanning Sonar -- A Theoretical Study. Int. Hydrog. Rev., 51(1), p. 61-80.
- Mackenzie, K.V. (1961). Bottom Reverberation for 530- and 1030-cps Sound in Deep Water. J. Acous. Soc. Am., v. 33 n. 11, p. 1498-1504.
- Mackenzie, K.V. and G. S. Yee (1961). Long-Range Shallow-Water Reverberation. U.S. Navy Electronics Laboratory, R&D Report 1072.
- Mellon, R. H. (1976). A Nearfield Model of the Parametric Radiator Part II: Saturated Source Levels. Naval Underwater Systems Center, TM No. PA4-53-76.
- Moffett, M. B. and R. H. Mellen (1977). Model for Parametric Acoustic Sources. J. Acous. Soc. Am., v. 61, n. 2, p. 325-337.
- Moss, G.J., and G. M. Walsh (1970). Correlation Signal Processing for Depth Sounding. Journal of the Institute of Navigation, v. 17, n. 2, p. 158-163.
- Schulkin, M., and R. Shaffer (1964). Backscattering of Sound from the Sea Surface. J. Acous. Soc. Am. 36:1699 (1964).
- Urick, R. J. (1967). Principles of Underwater Sound for Engineers. McGraw-Hill, New York, N.Y.
- Weinburn, H. (1973). Navy Interim Surface Ship Model (NISSM) II. Naval Underwater System Center. Technical Report 4527.

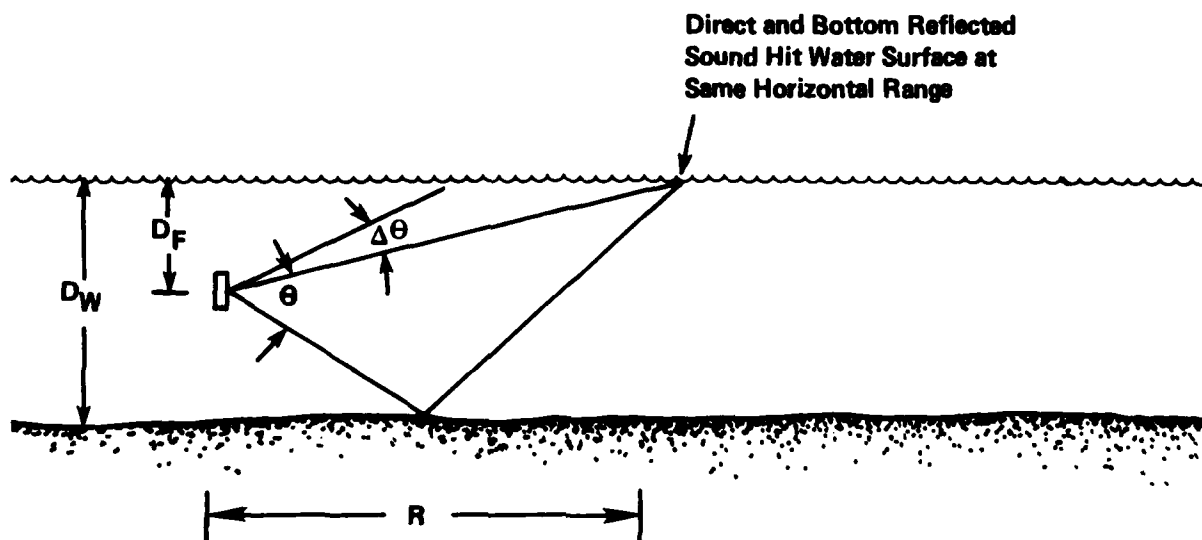


Figure 1. Geometry for Calculation of Required Beamwidth



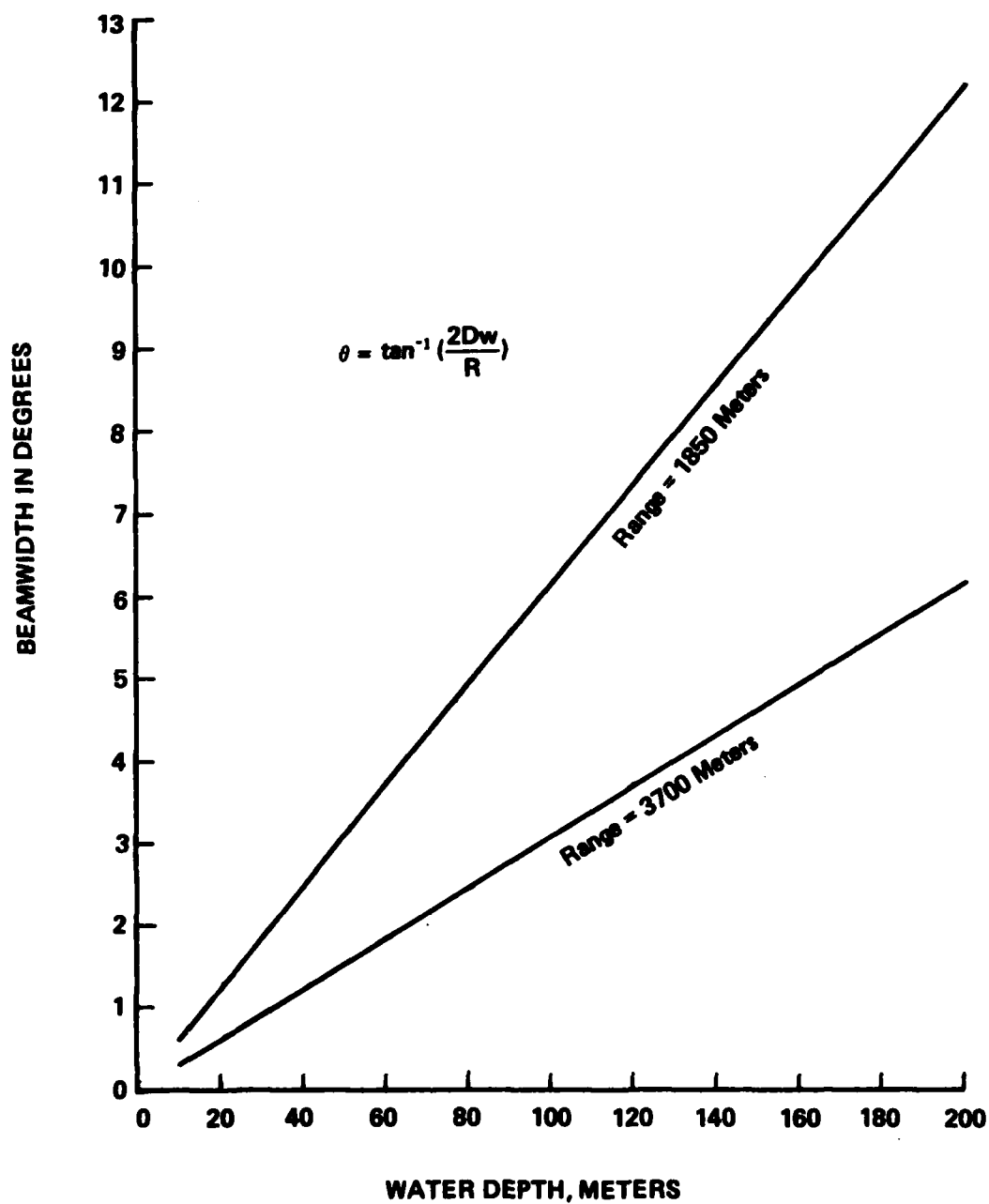


Figure 2. Lower Bound on Required Beamwidth for Constant Depth Isovelocity Water

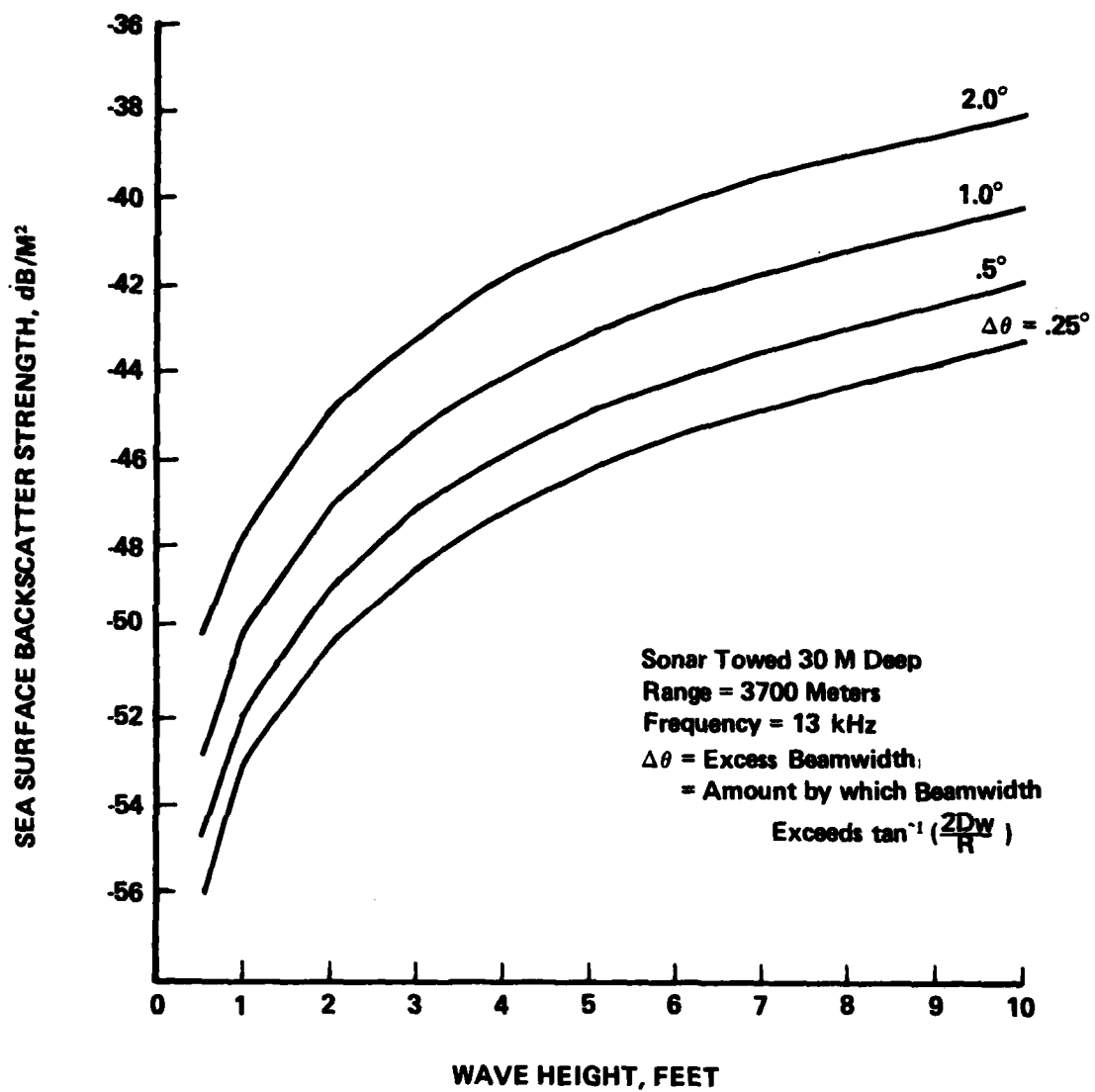


Figure 3. Sea Surface Backscatter Strength Resulting from Beamwidths in Excess of Calculated Lower Bound

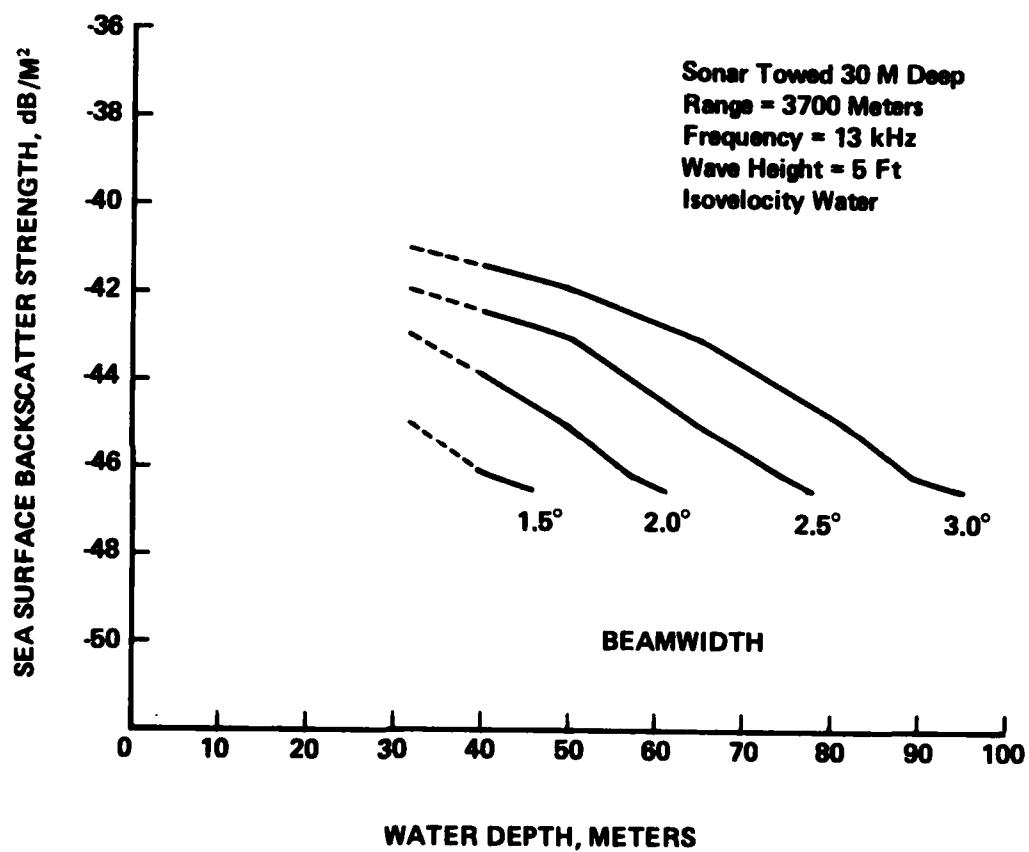


Figure 4. Sea Surface Backscatter Strength as a Function of Beamwidth and Water Depth



Figure 5. EDO-65 Transducer

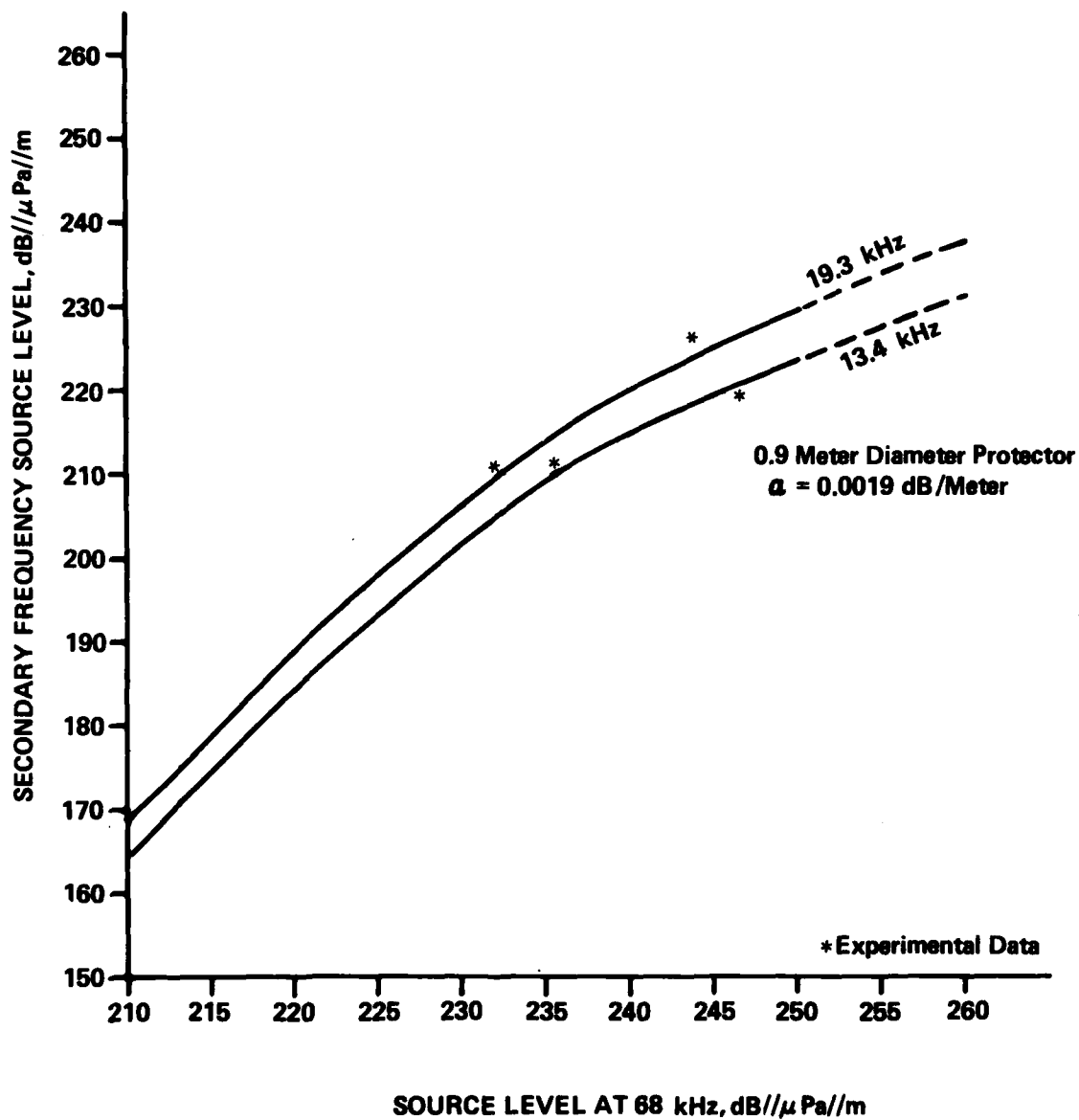


Figure 6. Parametric Source Level

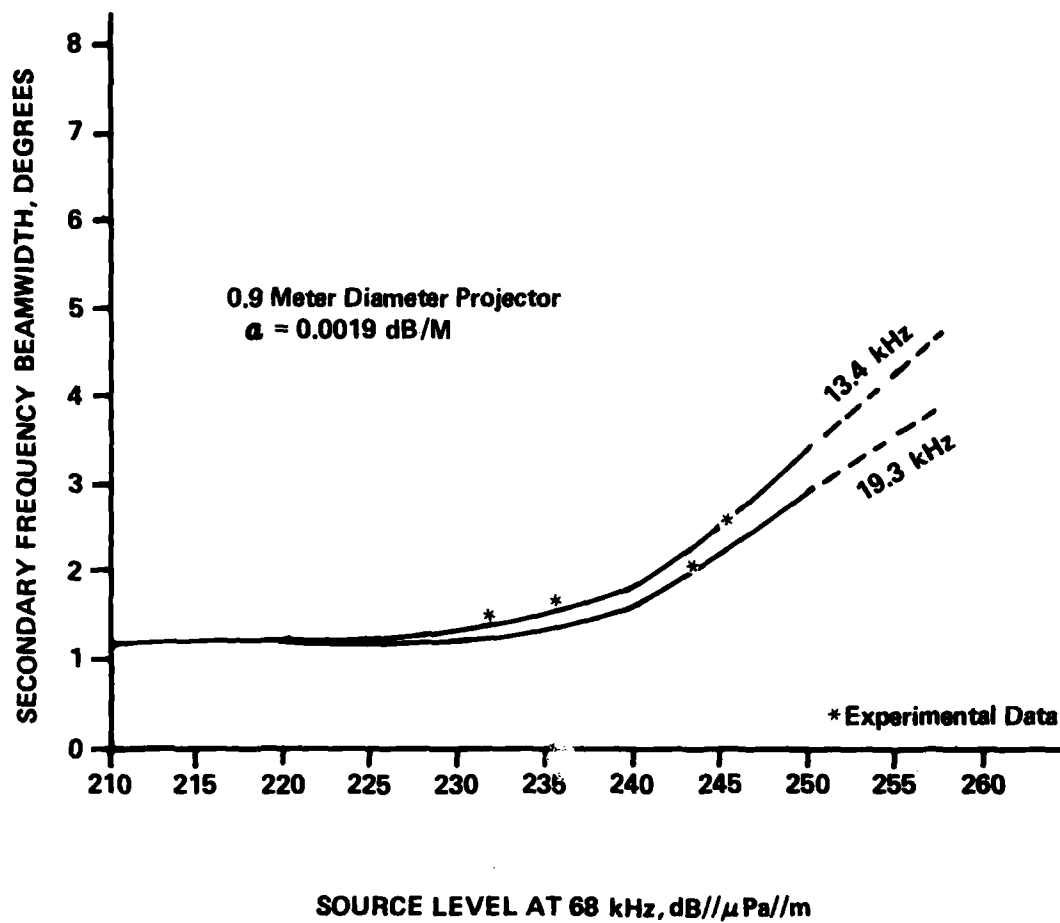


Figure 7. Parametric Beamwidth

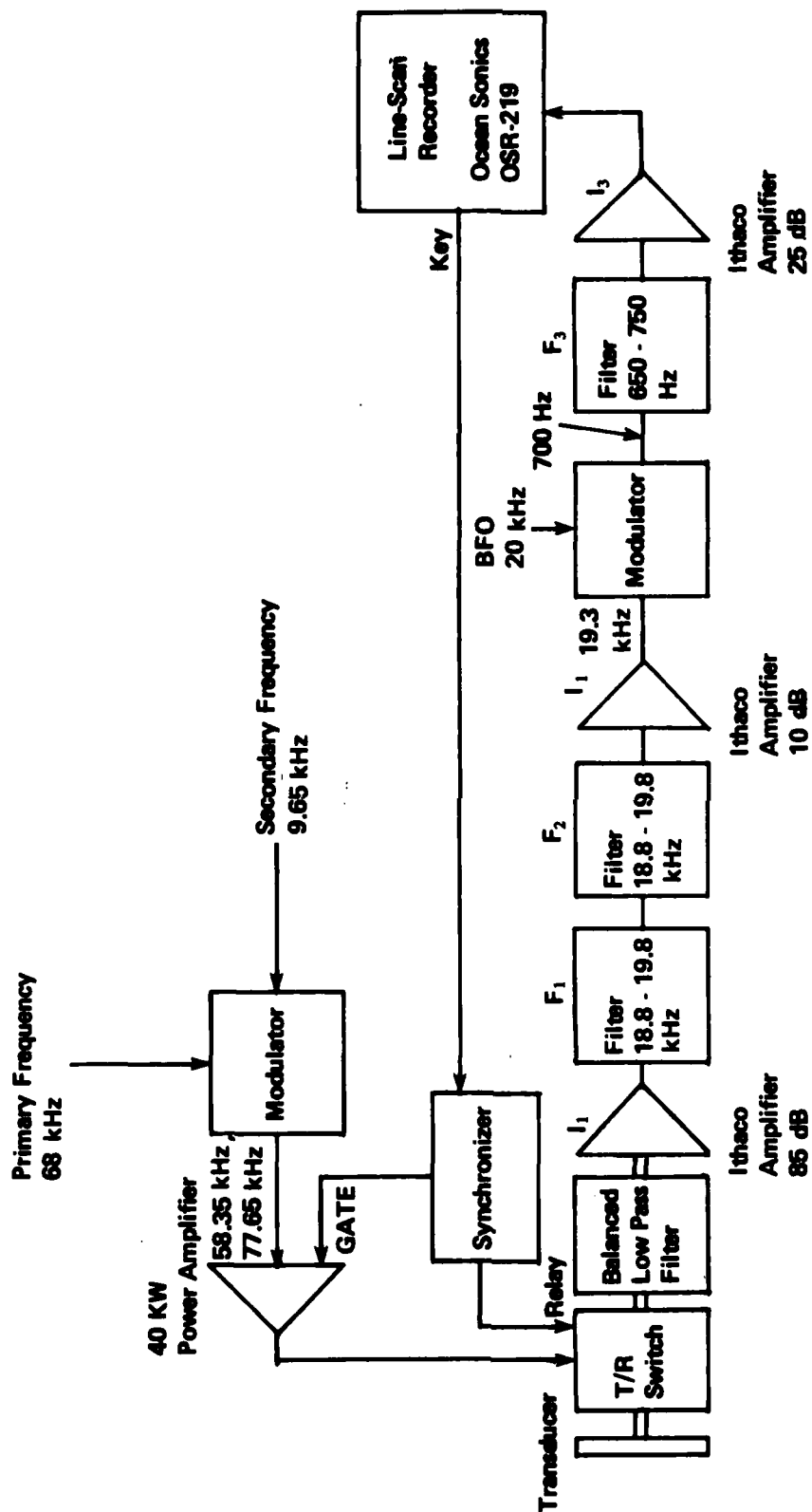


Figure 8. Pulsed CW Operation

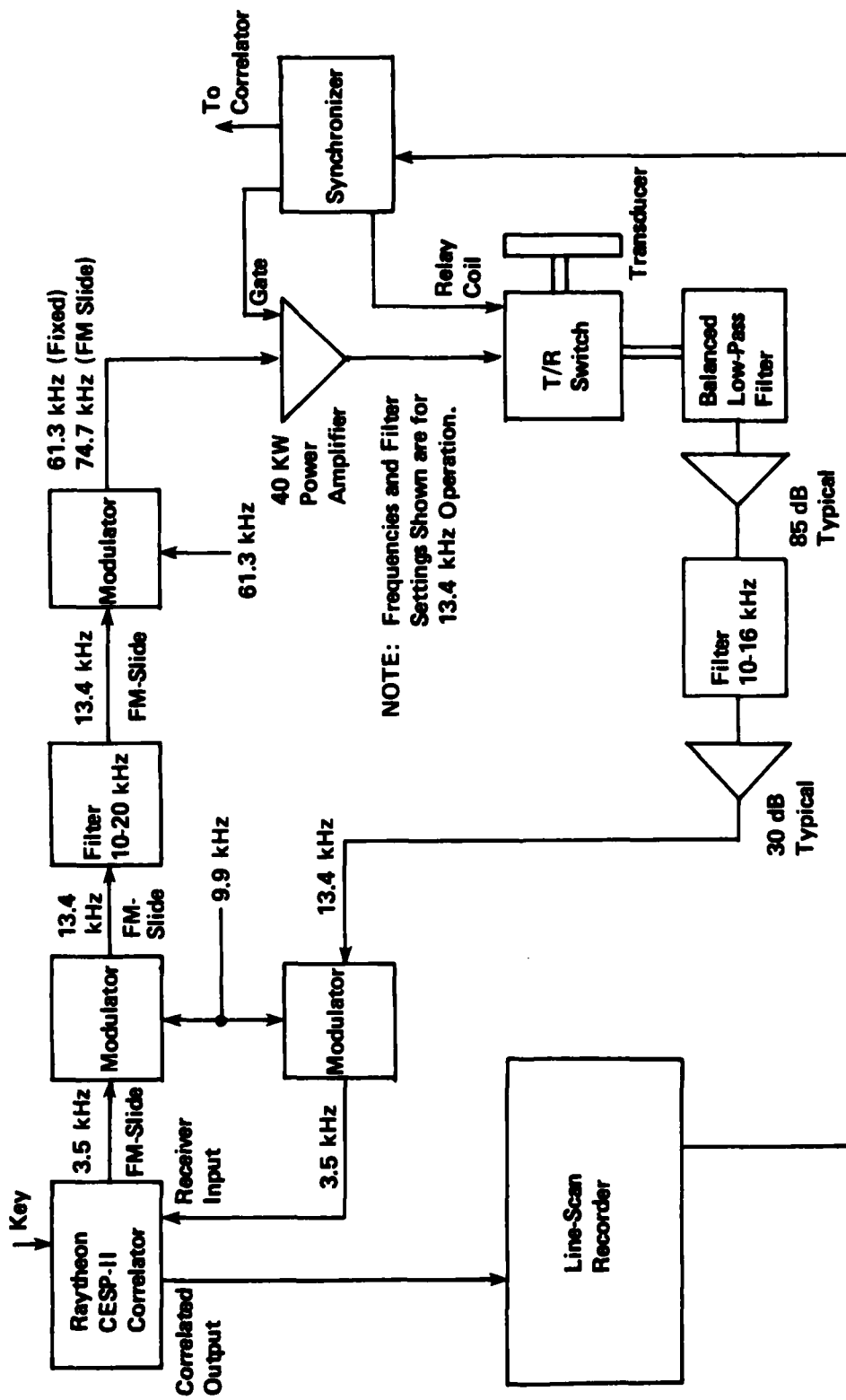


Figure 9. Correlation Operation



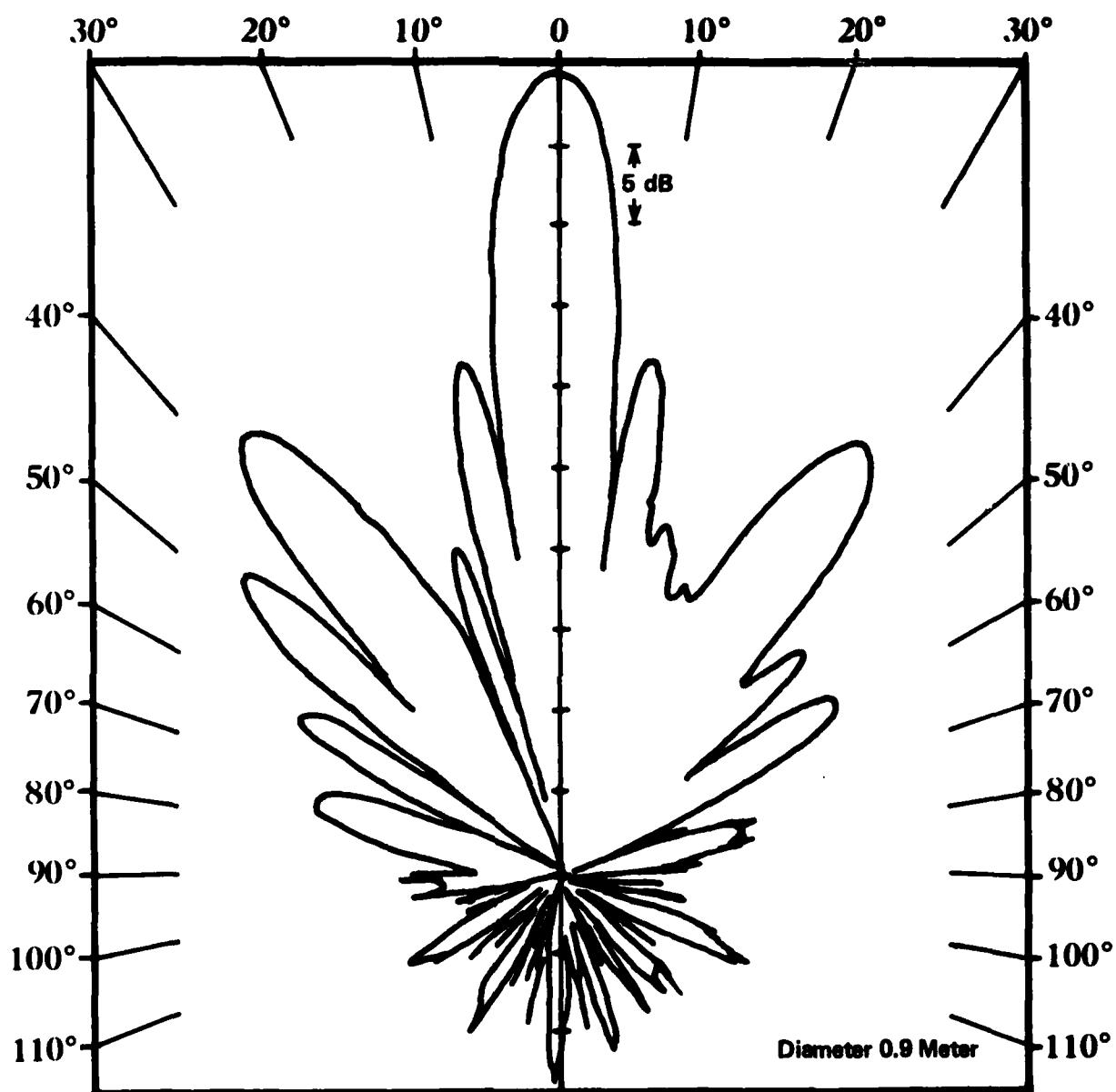
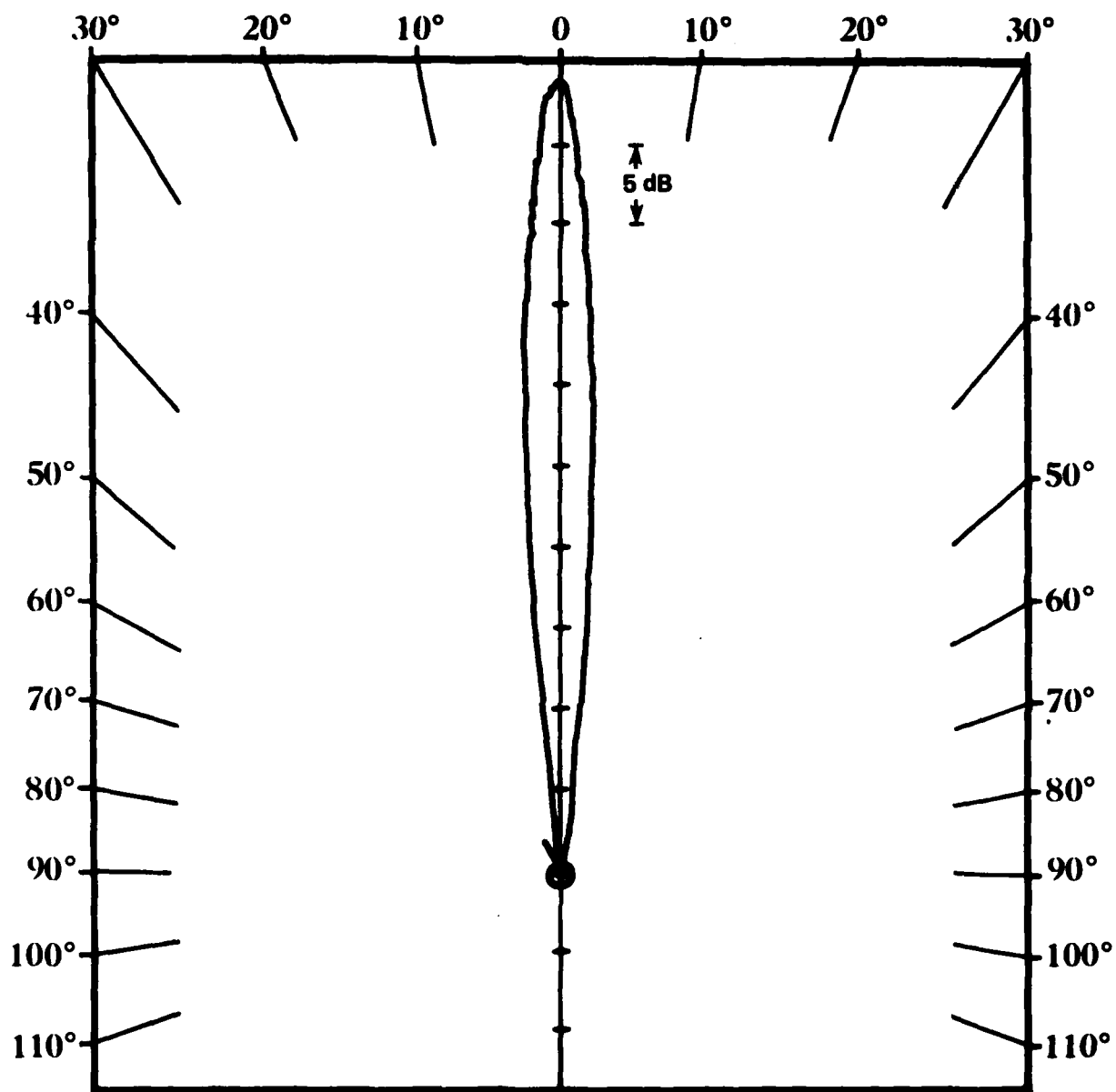


Figure 10. Conventional Beam Pattern at 13.4 kHz



Diameter 0.9 Meter  
Primary Source Level 246.4 dB// $\mu$ Pa//m at 68 kHz  
Secondary Source Level 218.9 dB// $\mu$ Pa//m at 13.4 kHz

Figure 11. Parametric Beam Pattern at 13.4 kHz

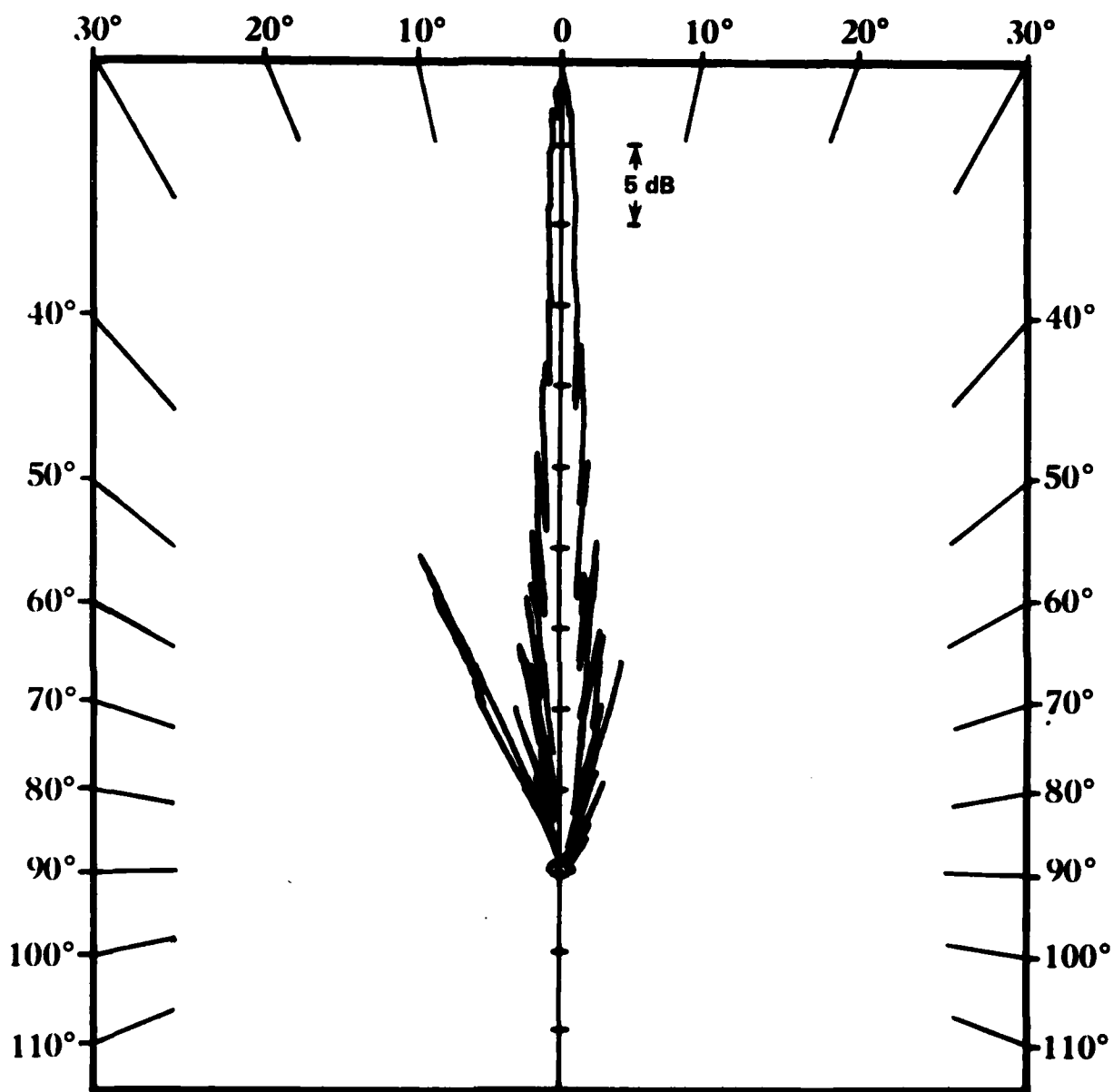
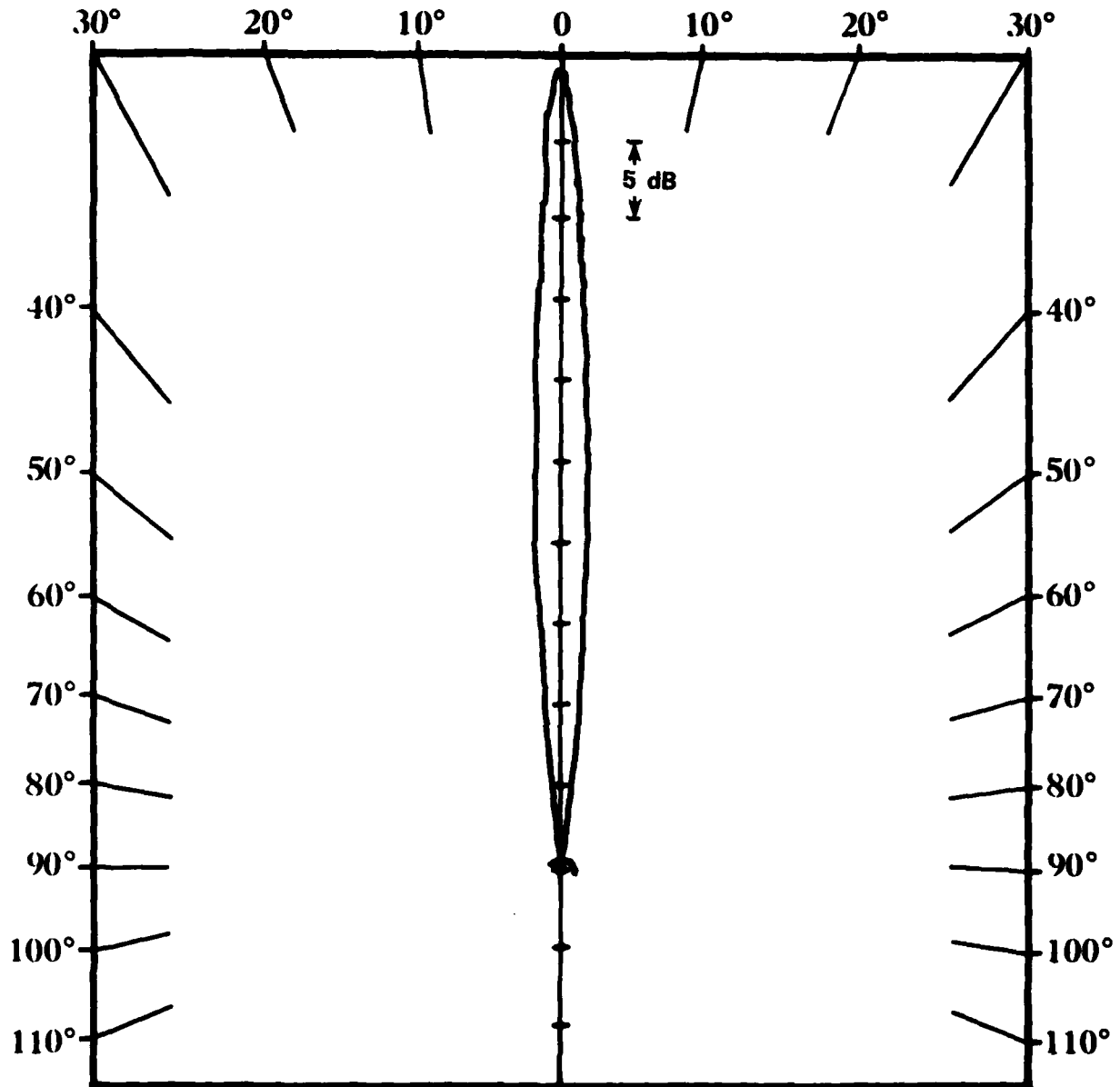


Figure 12. Conventional Beam Pattern at 68 kHz



Diameter 0.9 Meter  
 Primary Source Level 235.5 dB// $\mu$ Pa//m at 68 kHz  
 Secondary Source Level 203.9 dB// $\mu$ Pa//m at 13.4 kHz

Figure 13. Reduced Power Parametric Beam Pattern at 13.4 kHz

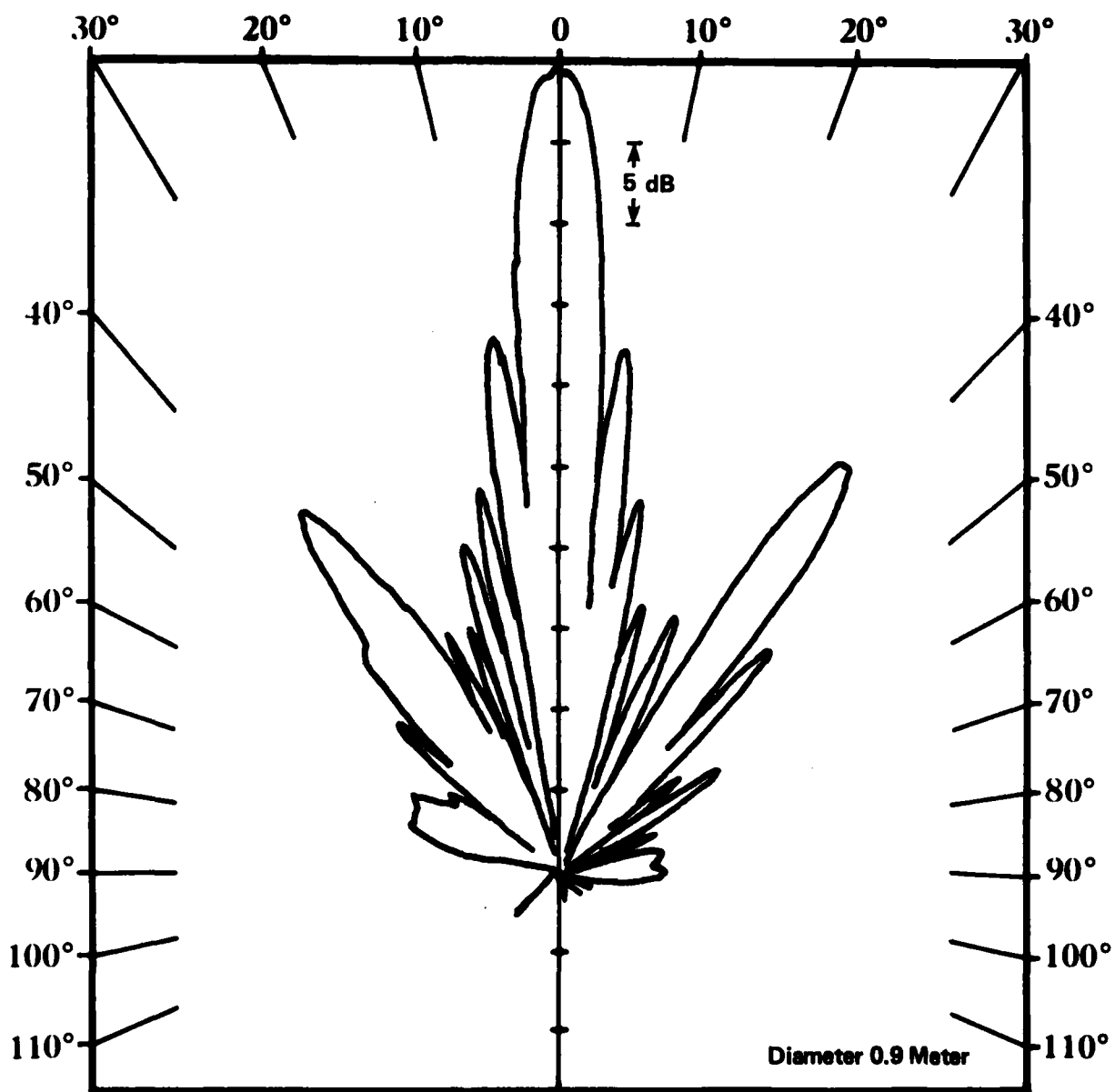
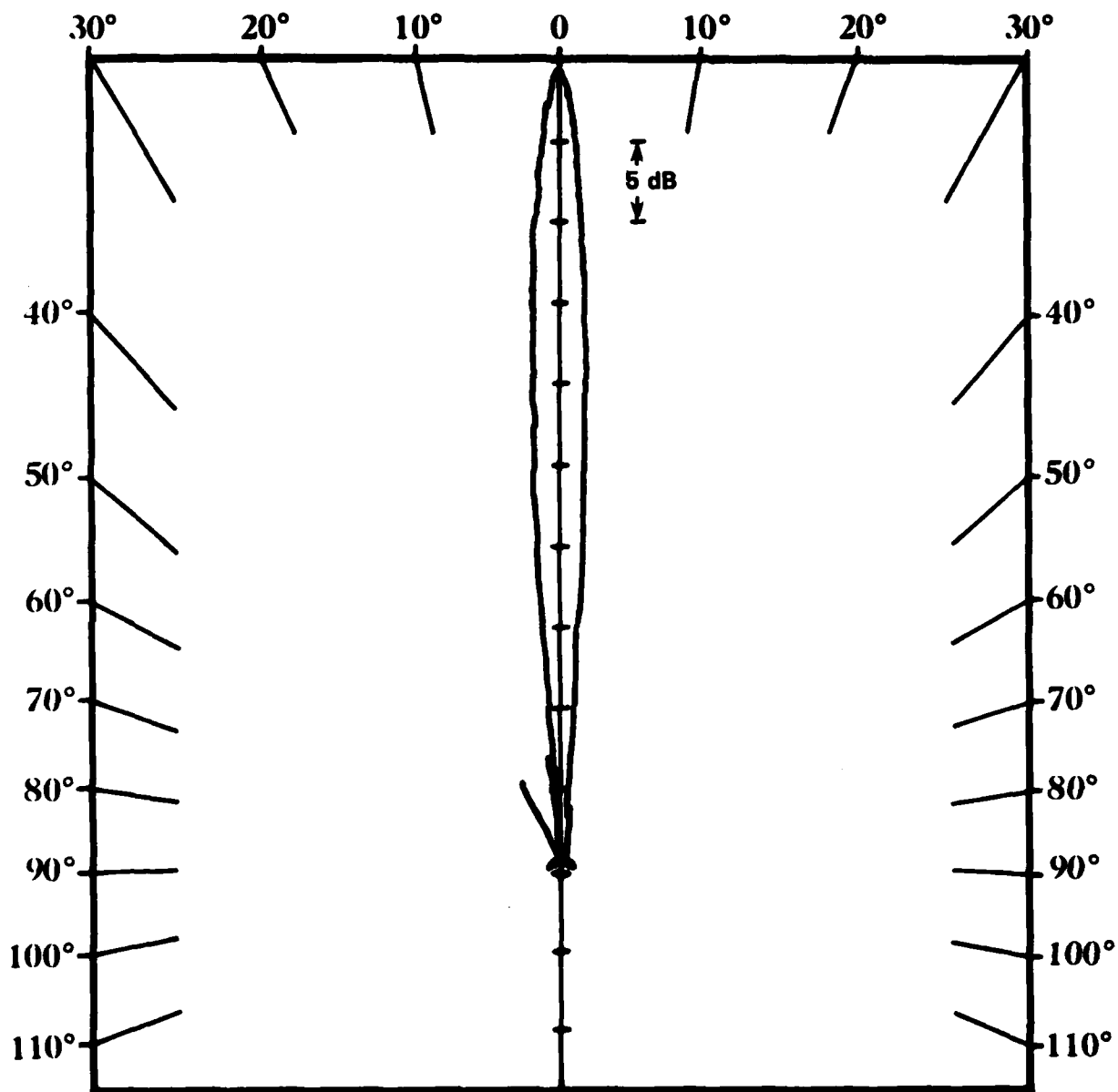


Figure 14. Conventional Beam Pattern at 19.3 kHz



Diameter 0.9 Meter  
Primary Source Level 243.5 dB //  $\mu$ Pa/m at 68 kHz  
Secondary Source Level 223.8 dB //  $\mu$ Pa/m at 19.3 kHz

Figure 15. Parametric Beam Pattern at 19.3 kHz



PULSE: 10MS CW  
ELEVATION ANGLE: 0.3° UP  
RANGE: 6 SECONDS

Figure 16. Pulsed CW Scan with a 6 Second Range

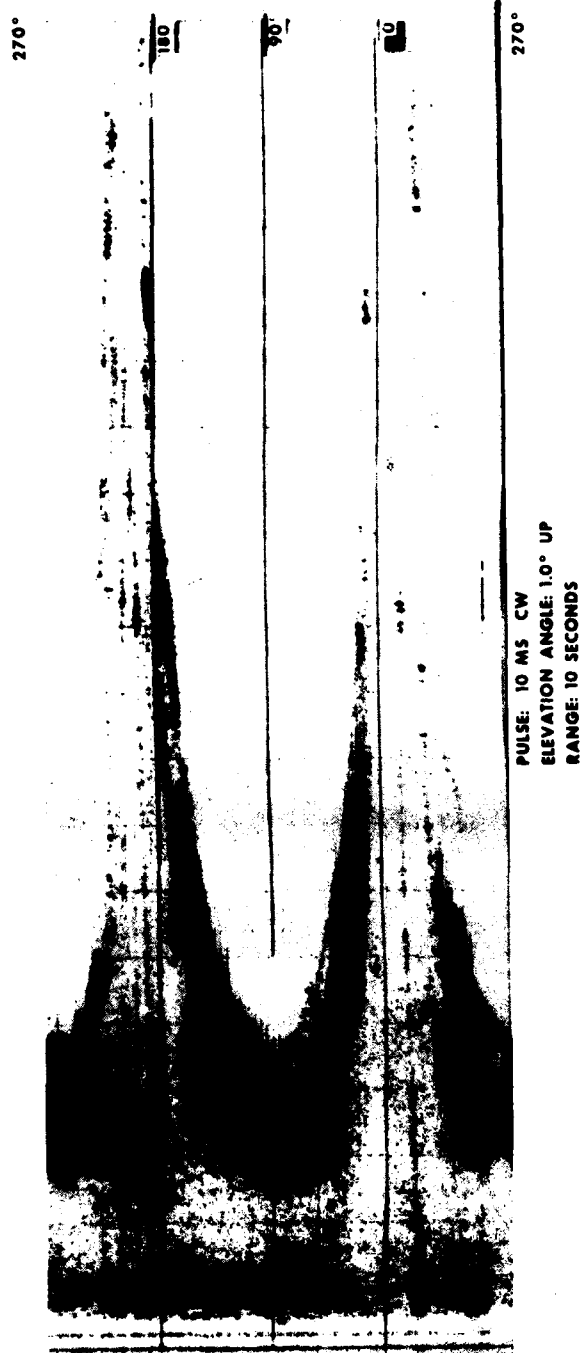
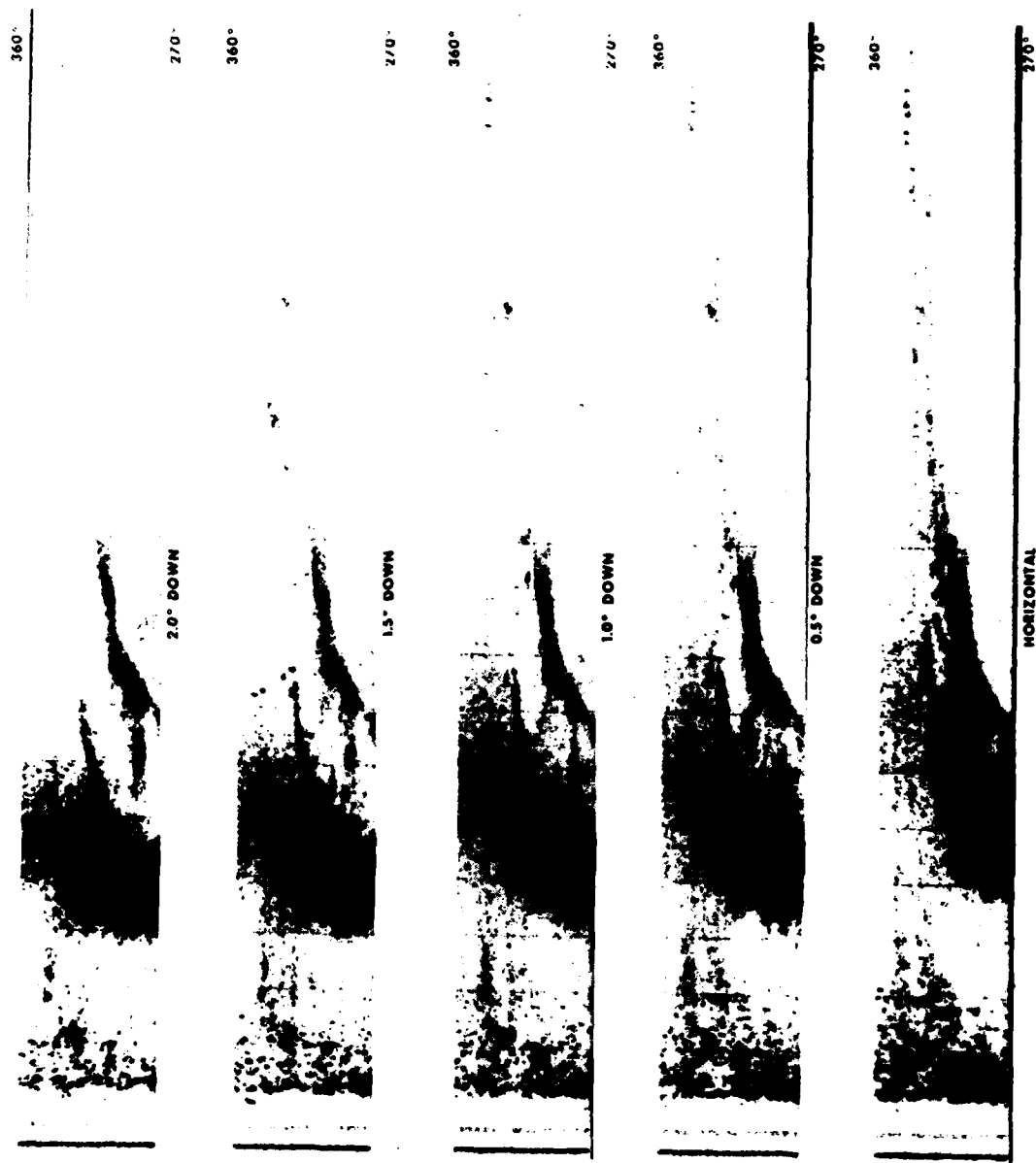


Figure 17. Pulsed CW Scan with a 10 Second Range





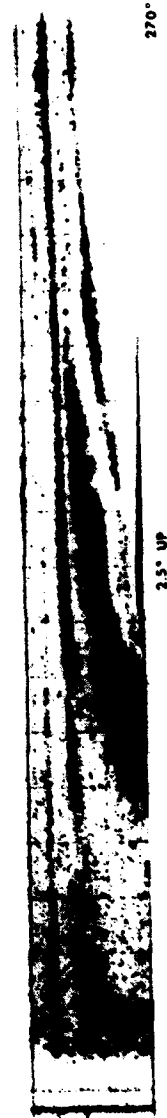
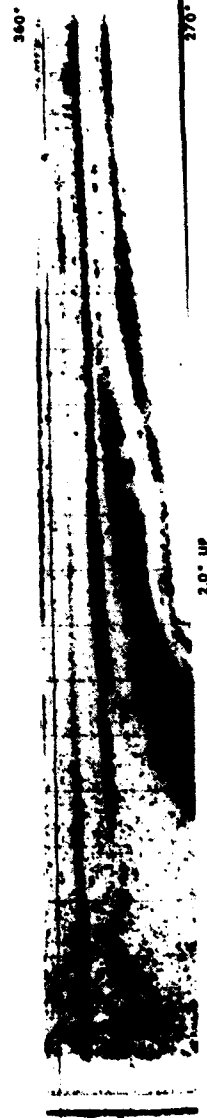
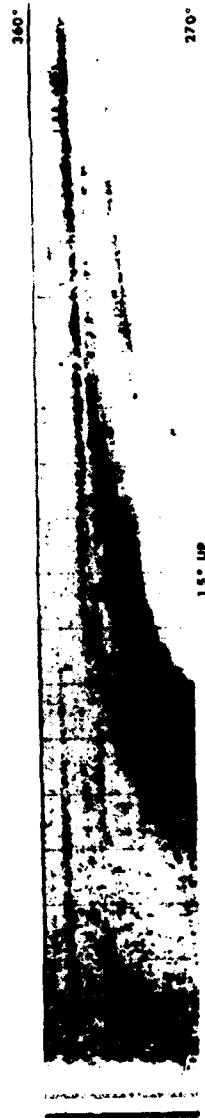


Figure 19. Effect of Elevation Angle, 1.0° up to 2.5° up

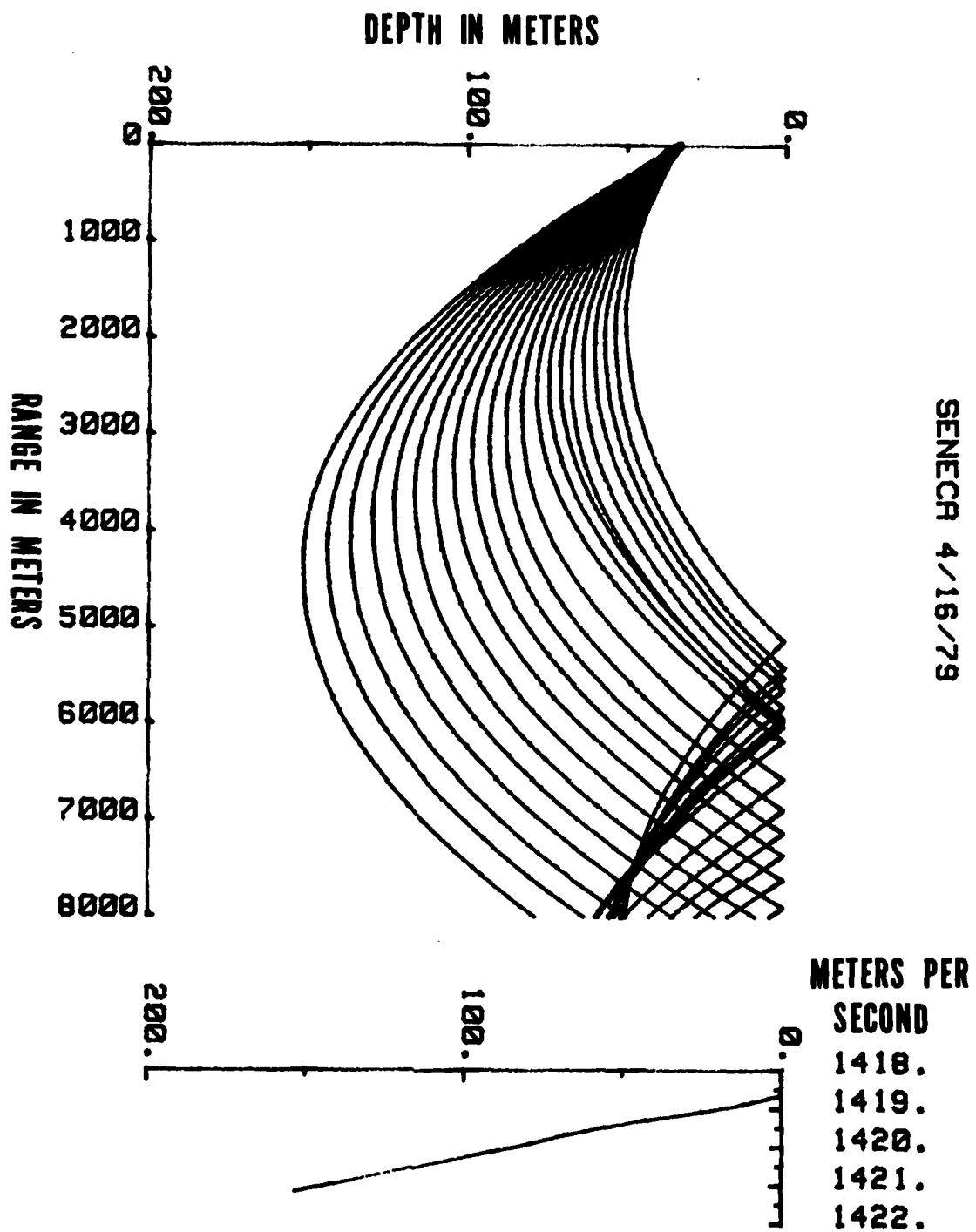


Figure 20. Ray Trace for Beam Directed 2.0° Below Horizon

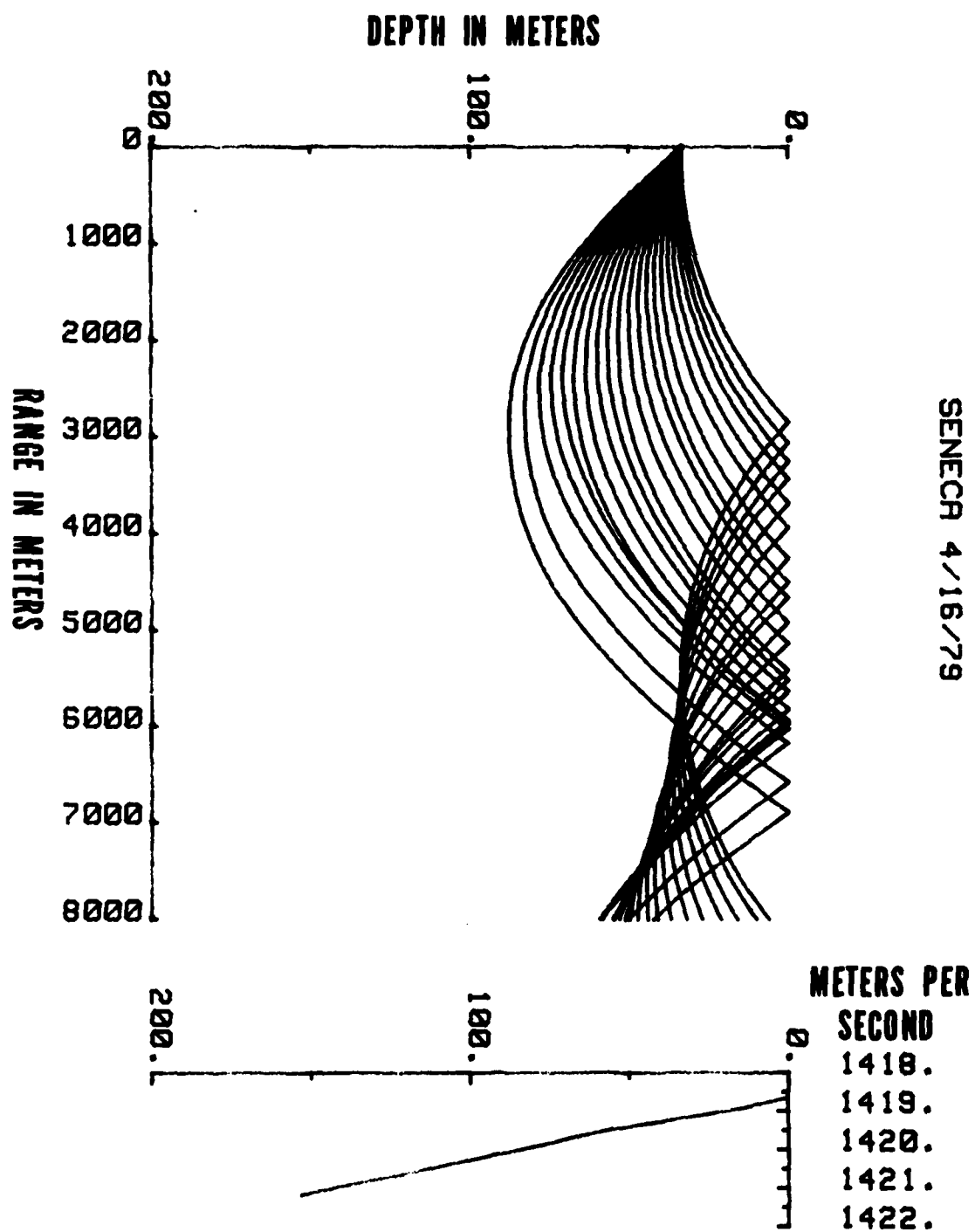


Figure 21. Ray Trace for Beam Directed 1.0° Below Horizon

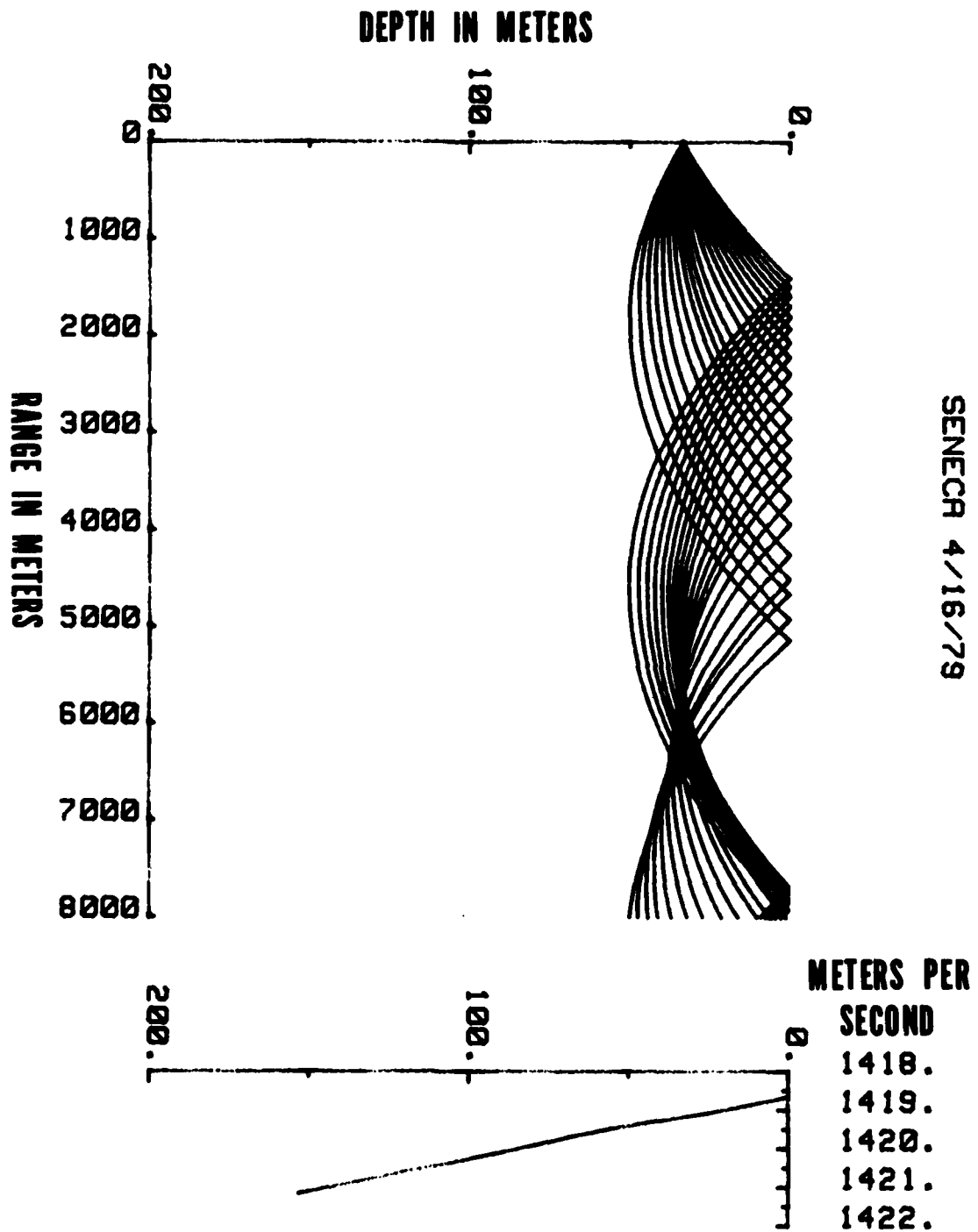


Figure 22. Ray Trace for Horizontal Beam

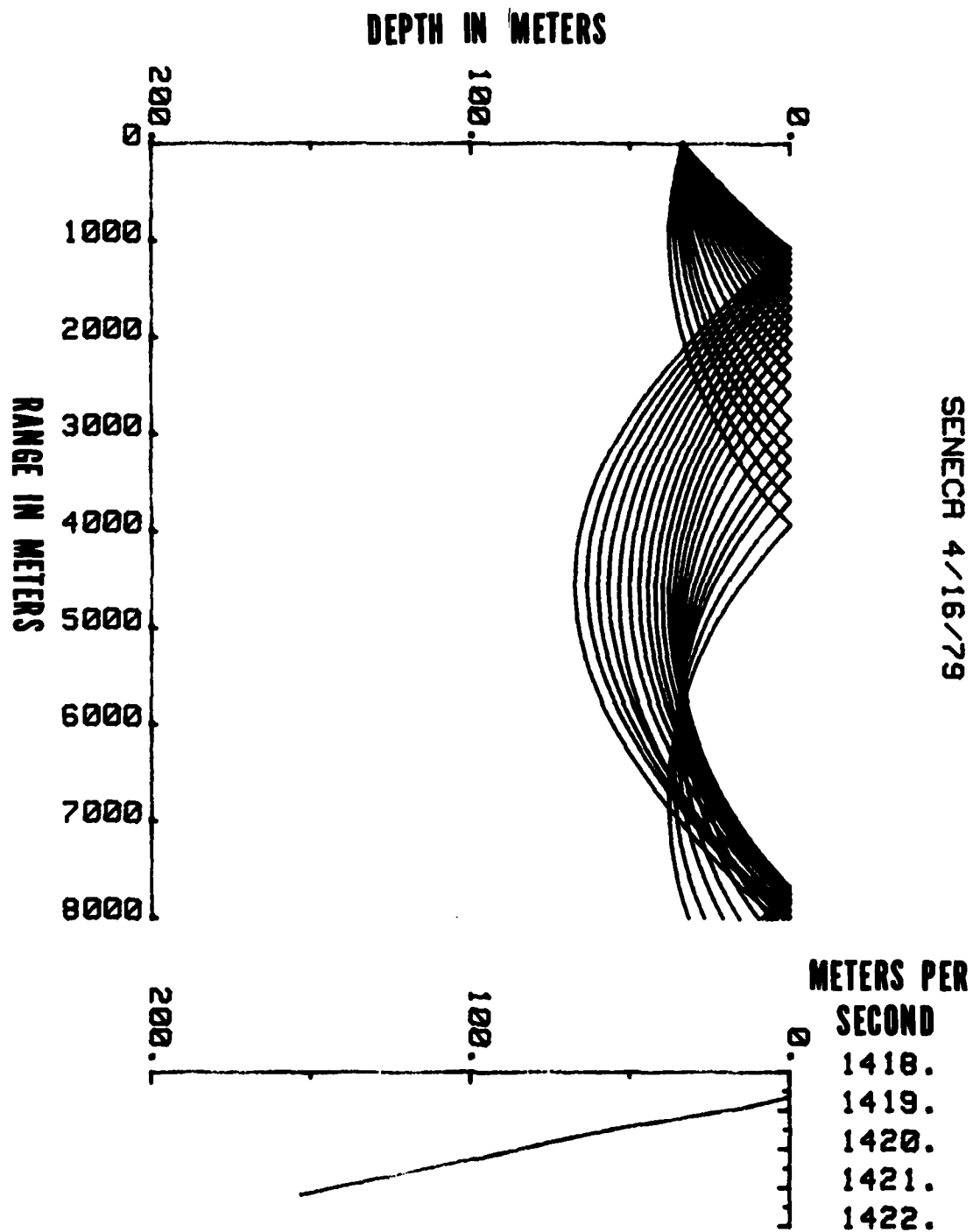


Figure 23. Ray Trace for Beam Directed 0.5° Above Horizon

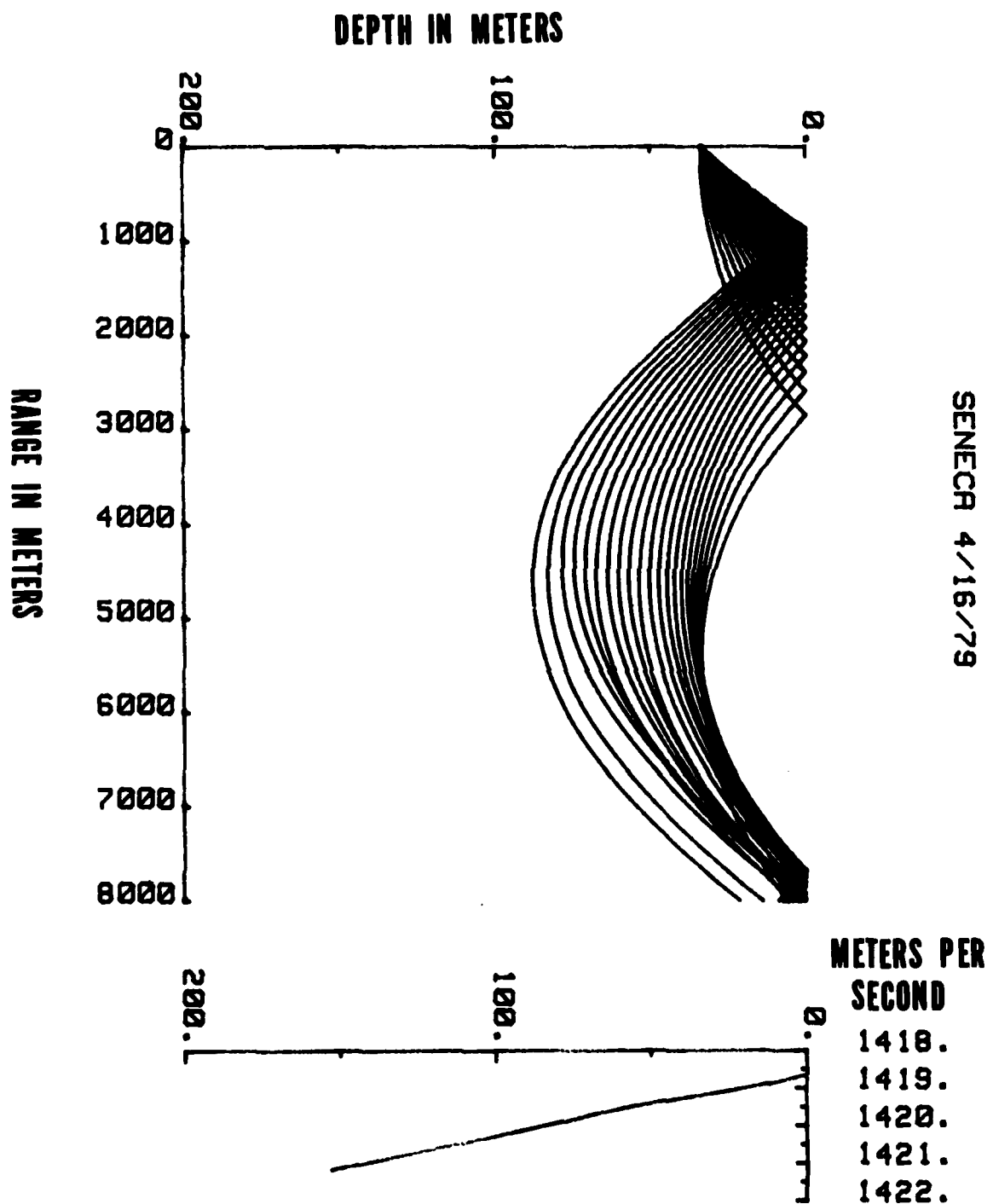


Figure 24. Ray Trace for Beam-Directed 1.0° Above Horizon

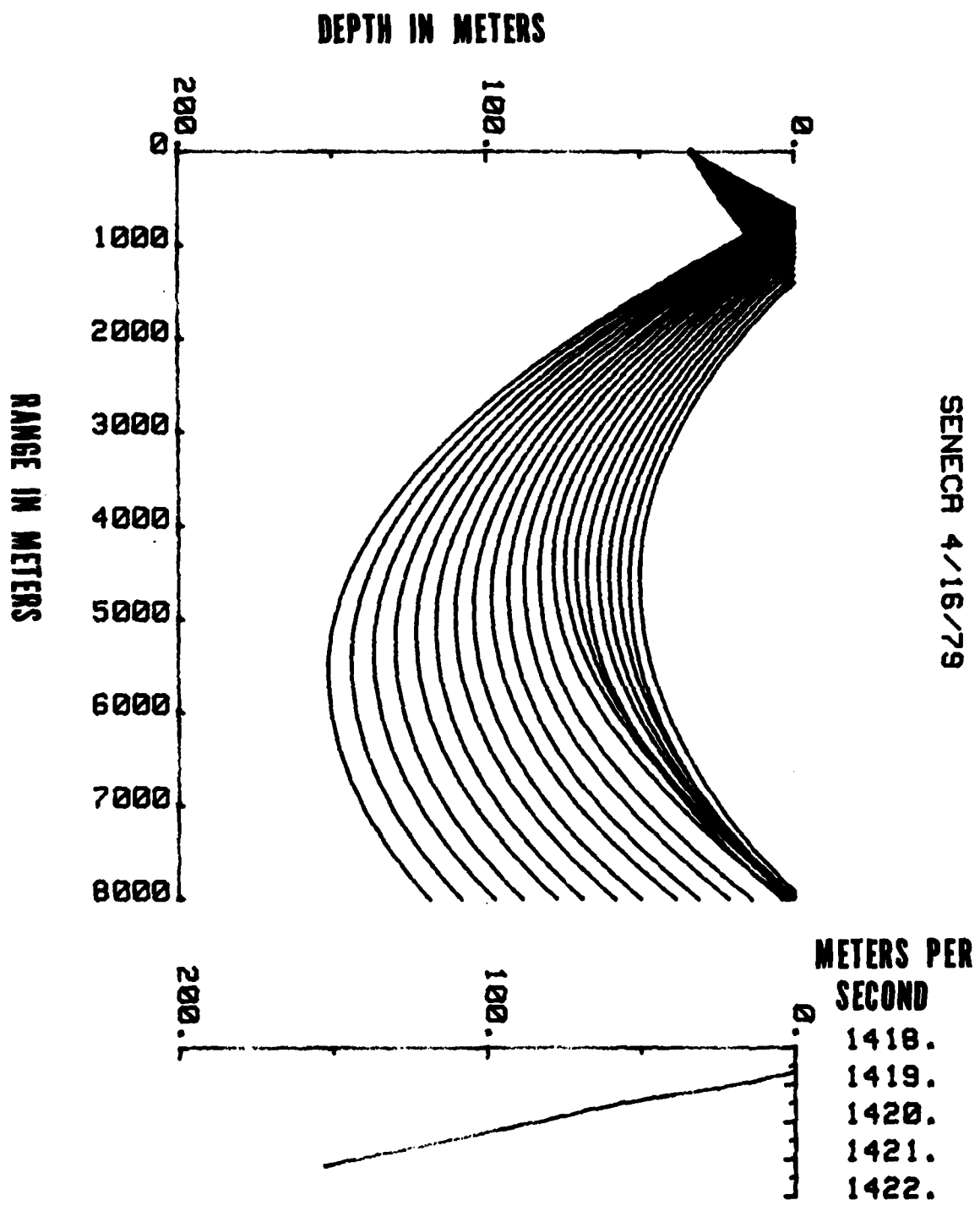
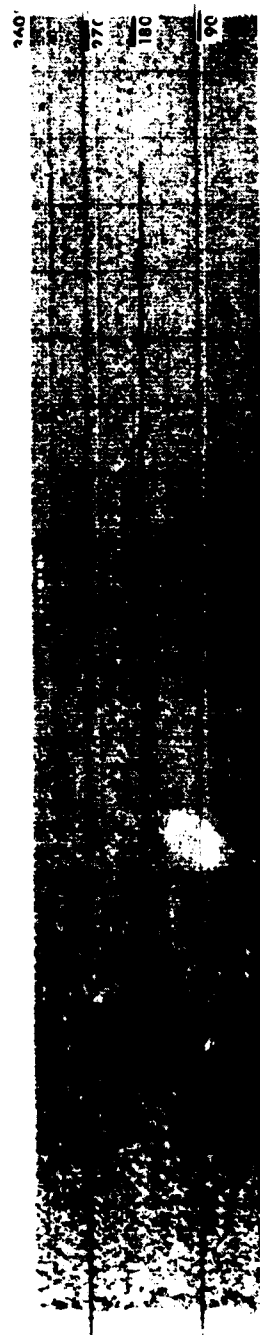


Figure 25. Ray Trace for Beam Directed 2.0° Above Horizon





PULSE: 100 MS 2MHz FM SLIDE  
 ELEVATION ANGLE 1.0° UP  
 RANGE: 10 SECONDS

Figure 26. Results of Correlation Operation

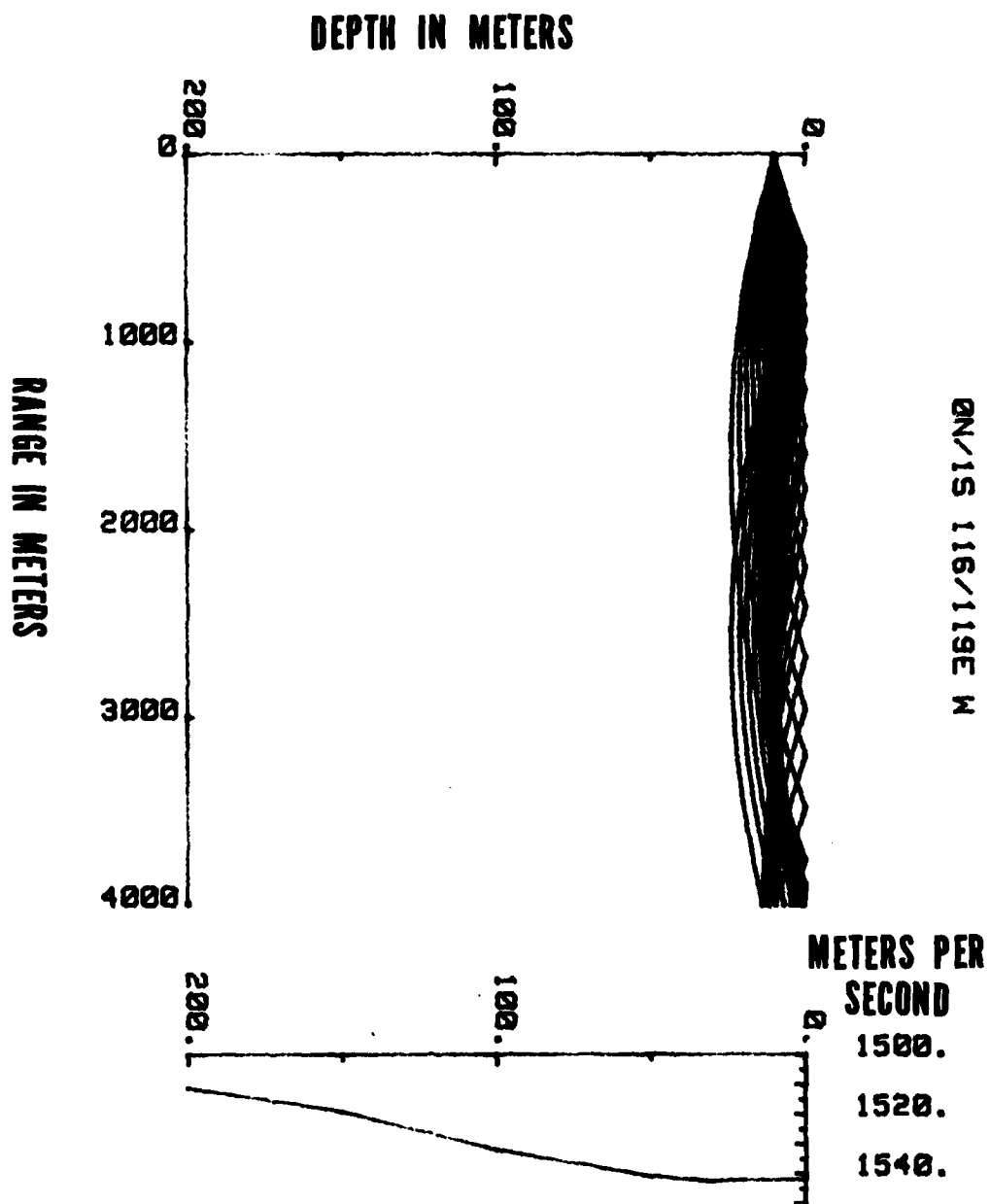


Figure 27. Ray Trace for Makassar Strait, Positive Gradient, 10 Meter Source Depth

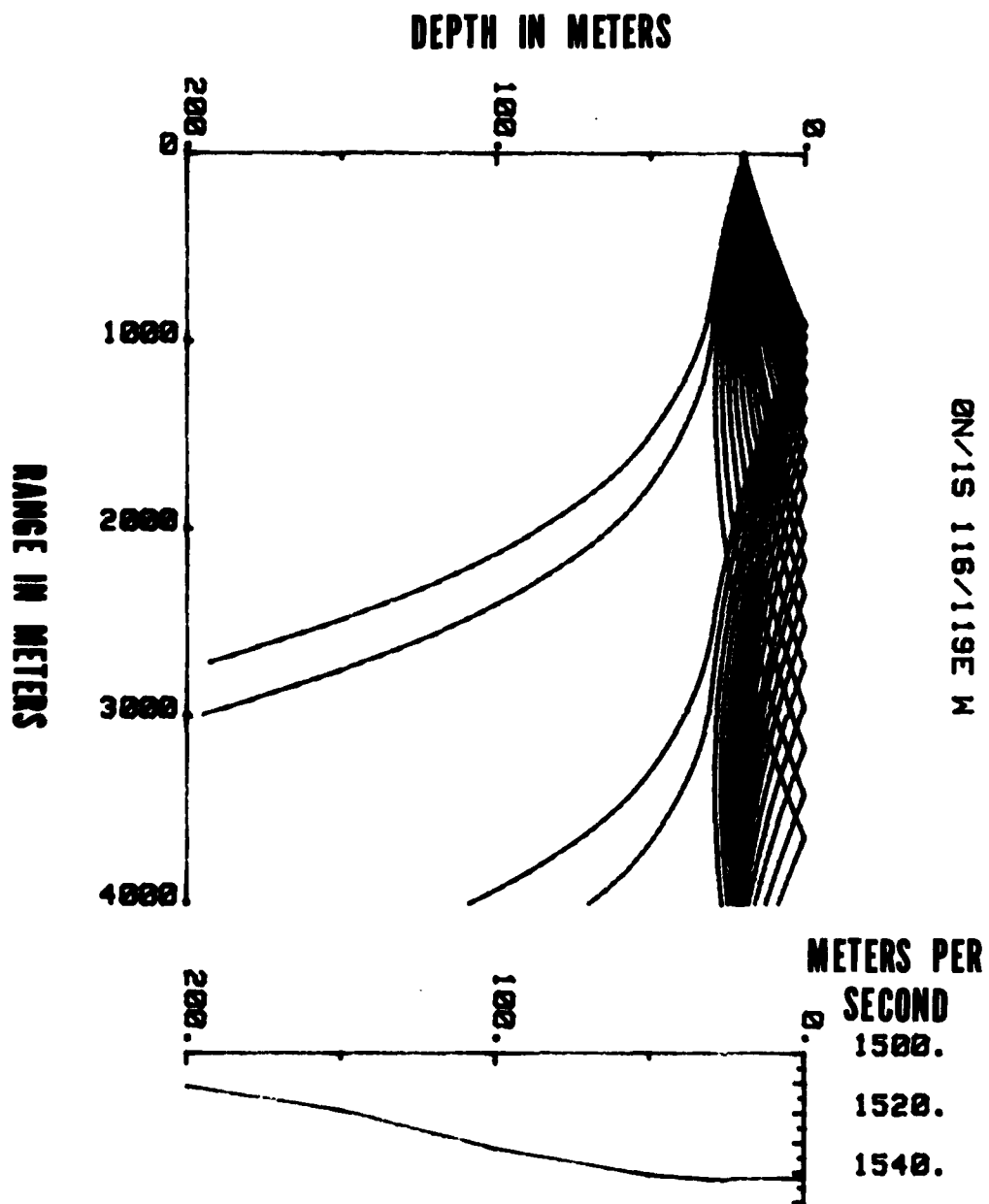


Figure 28. Ray Trace for Makassar Strait, Positive Gradient, 20 Meter Source Depth

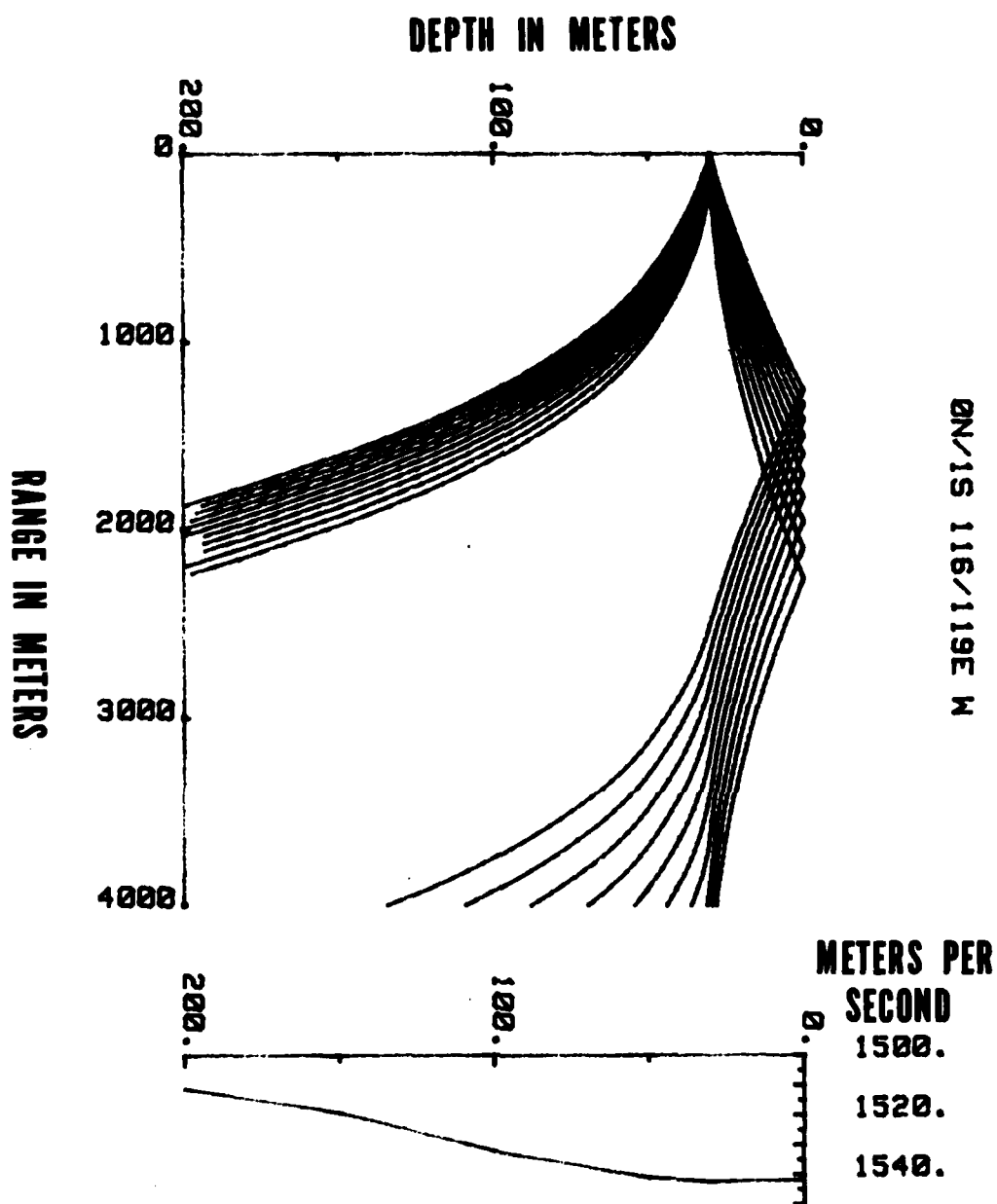


Figure 29. Ray Trace for Makassar Strait, Positive Gradient, 30 Meter Source Depth

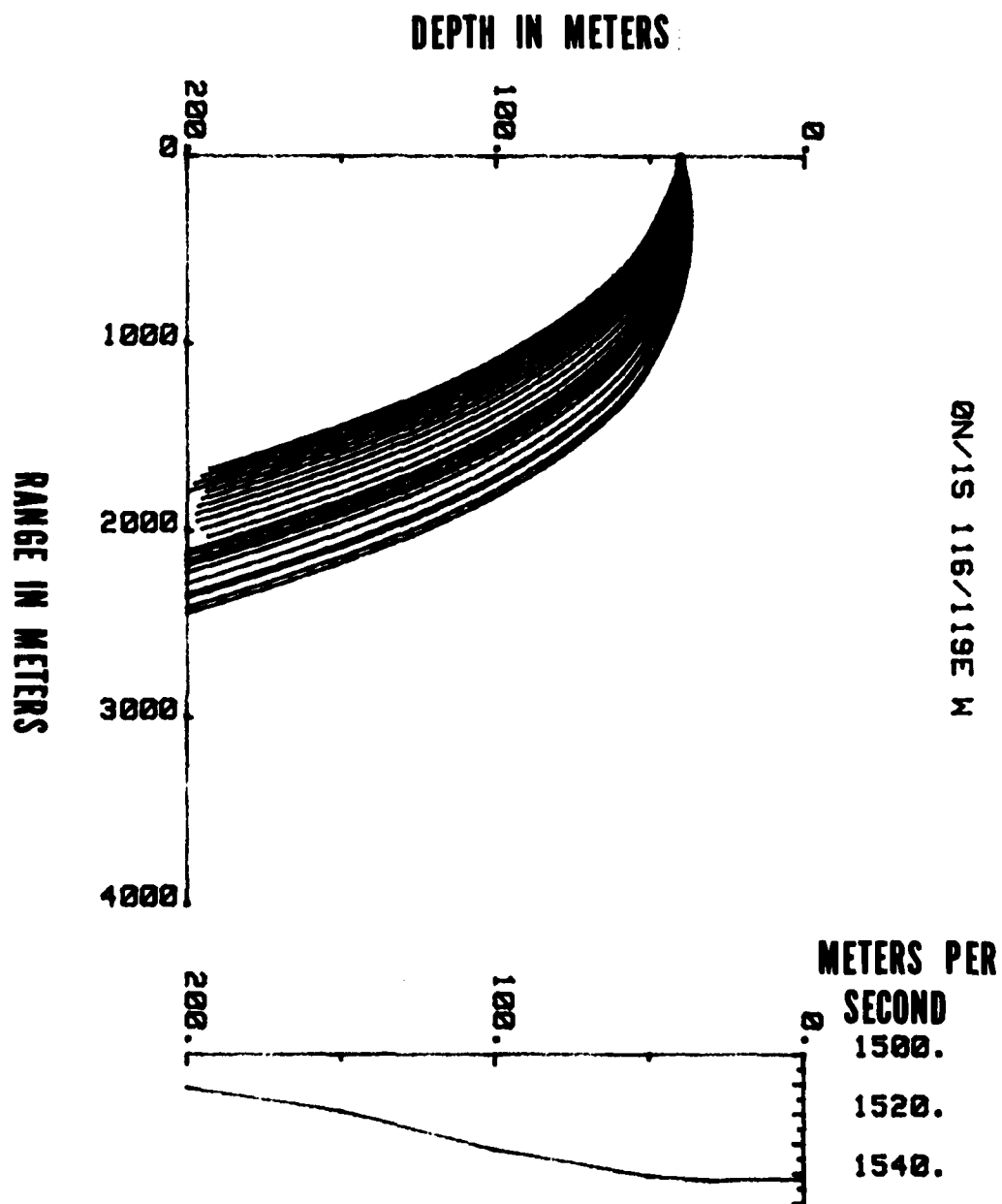


Figure 30. Ray Trace for Makassar Strait, Positive Gradient, 40 Meter Source Depth

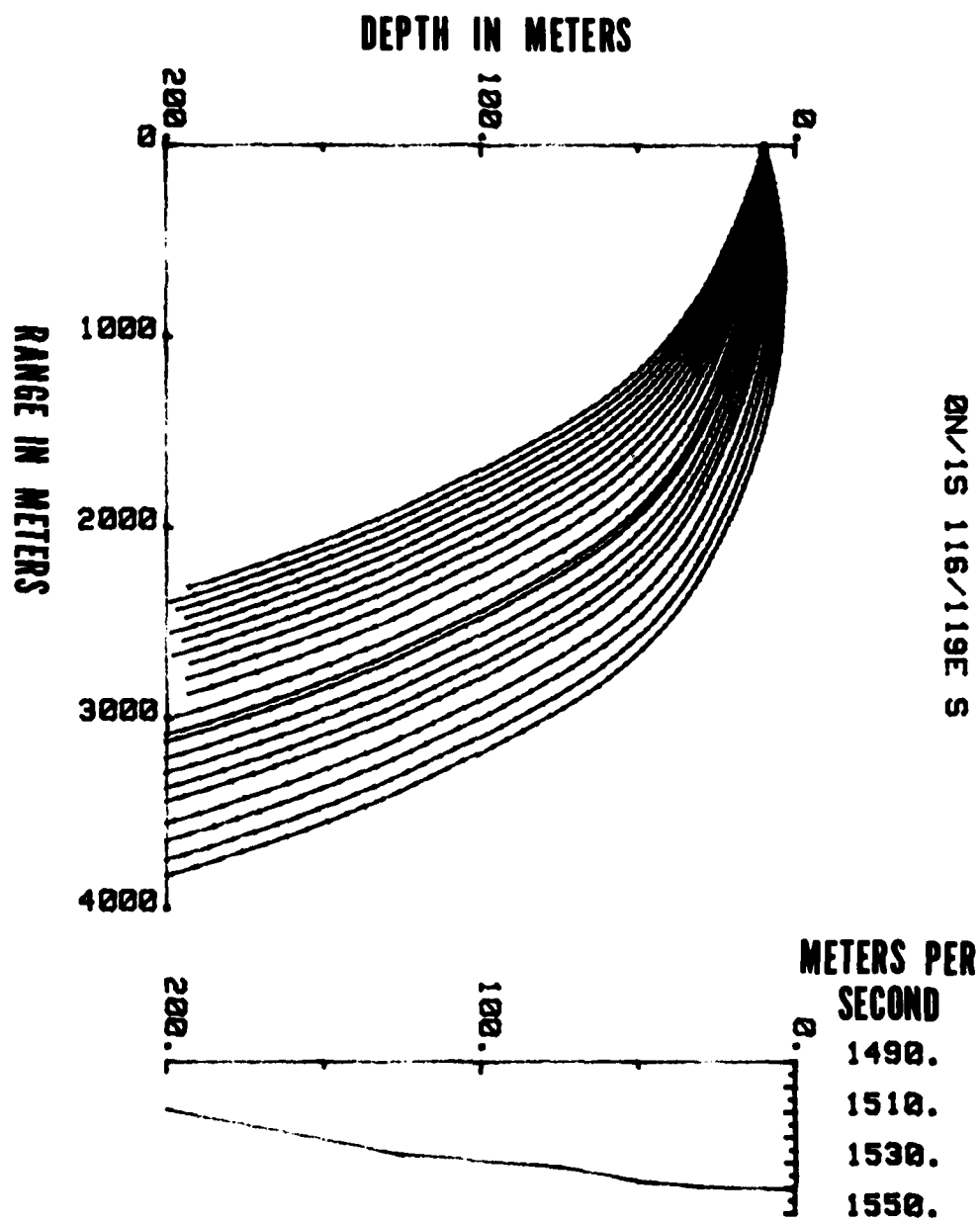


Figure 31. Ray Trace for Makassar Strait, Negative Gradient, 10 Meter Source Depth

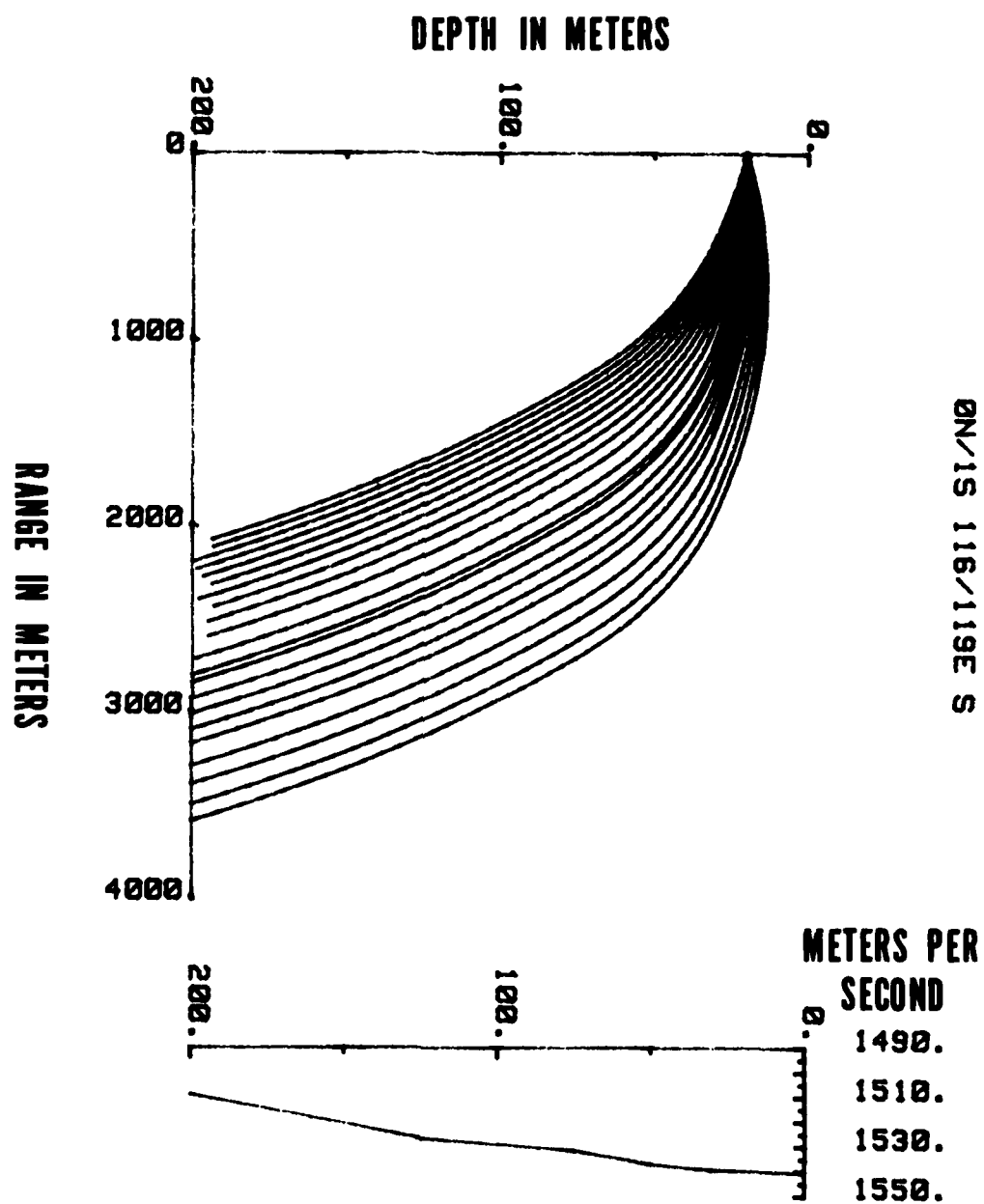


Figure 32. Ray Trace for Makassar Strait, Negative Gradient, 20 Meter Source Depth

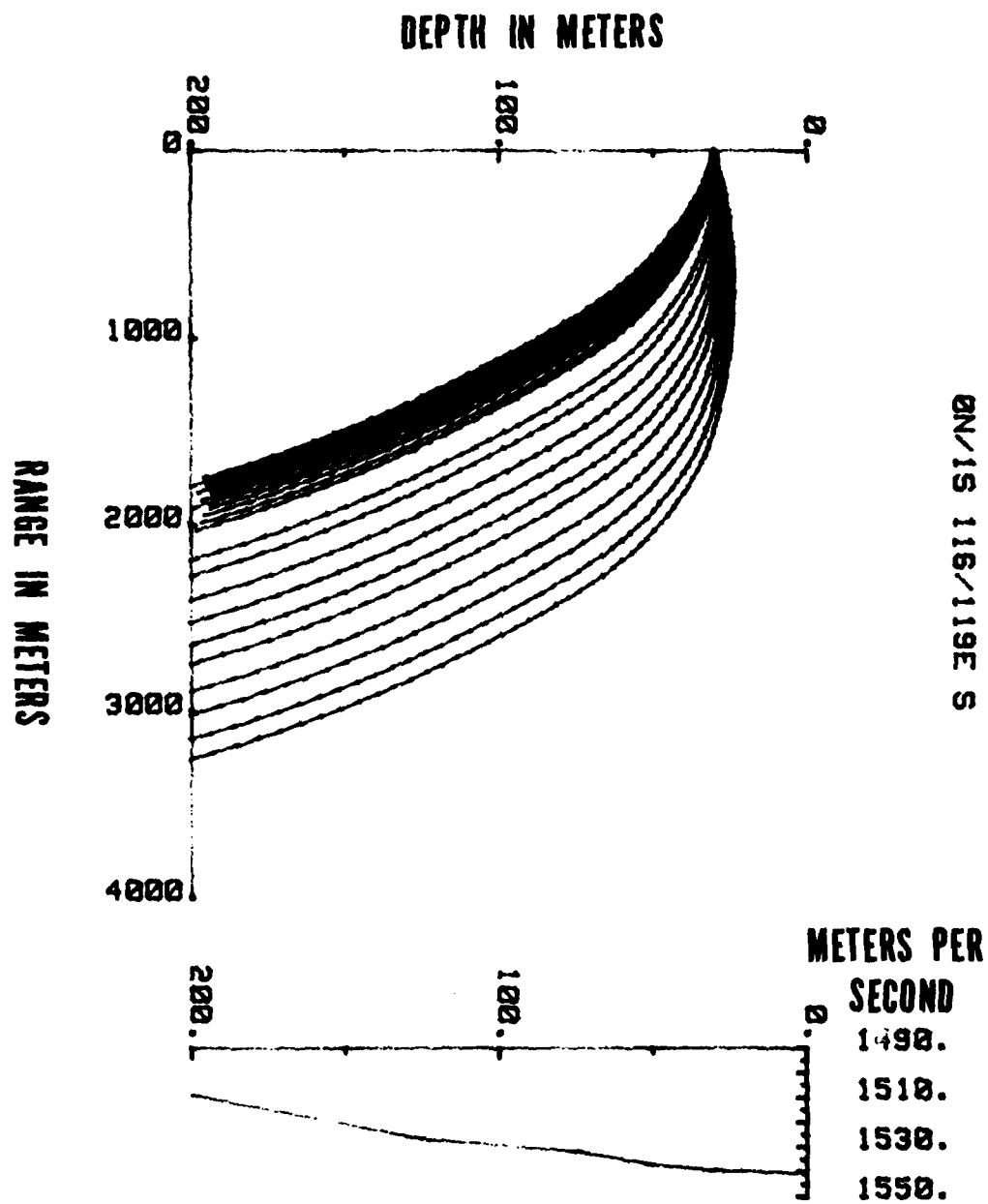


Figure 33. Ray Trace for Makassar Strait, Negative Gradient, 30 Meter Source Depth



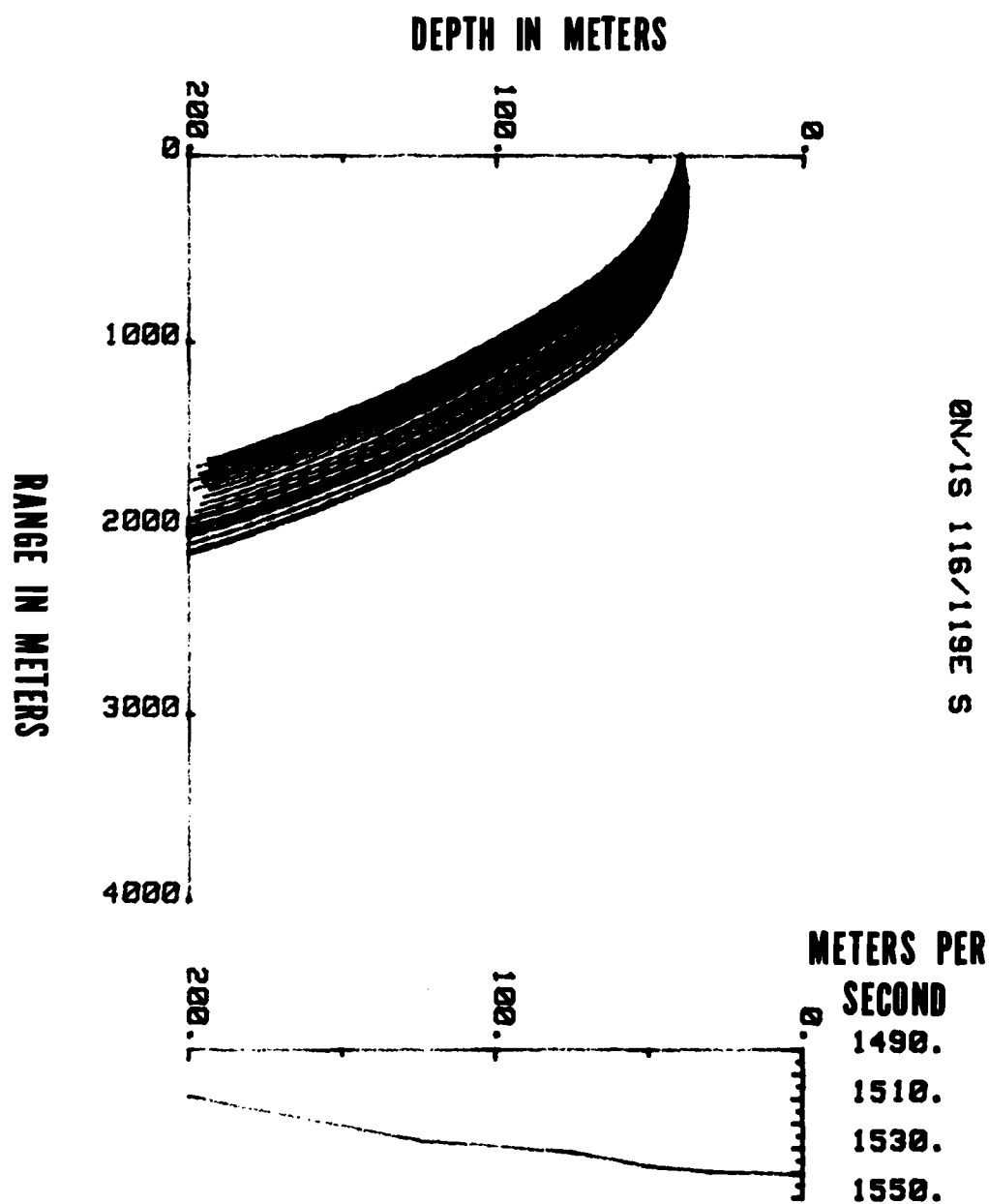


Figure 34. Ray Trace for Makassar Strait Negative Gradient, 40 Meter Source Depth

# UNCLASSIFIED

SECURITY CLASSIFICATION OF THIS PAGE (When Data Entered)

REPORT DOCUMENTATION PAGE		READ INSTRUCTIONS BEFORE COMPLETING FORM
1. REPORT NUMBER <b>NORDA Technical Note 53</b>	2. GOVT ACCESSION NO.	3. RECIPIENT'S CATALOG NUMBER
4. TITLE (and Subtitle) <b>Navigation Hazard Survey Sonar</b>		5. TYPE OF REPORT & PERIOD COVERED <b>Final Report</b>
7. AUTHOR(s) <b>George J. Moss, Jr.</b>		6. PERFORMING ORG. REPORT NUMBER
9. PERFORMING ORGANIZATION NAME AND ADDRESS <b>Naval Ocean Research and Development Activity Code 352 NSTL Station, Mississippi 39529</b>		8. CONTRACT OR GRANT NUMBER(s)
11. CONTROLLING OFFICE NAME AND ADDRESS <b>Naval Ocean Research and Development Activity Code 352 NSTL Station, Mississippi 39529</b>		10. PROGRAM ELEMENT, PROJECT, TASK AREA & WORK UNIT NUMBERS
14. MONITORING AGENCY NAME & ADDRESS (if different from Controlling Office)		12. REPORT DATE <b>March 1982</b>
		13. NUMBER OF PAGES <b>49</b>
		15. SECURITY CLASS. (of this report) <b>UNCLASSIFIED</b>
		15a. DECLASSIFICATION/DOWNGRADING SCHEDULE
16. DISTRIBUTION STATEMENT (of this Report) <b>Distribution Unlimited</b>		
<div style="border: 1px solid black; padding: 5px; display: inline-block;"> <b>DISTRIBUTION STATEMENT A</b>            Approved for public release;            Distribution Unlimited         </div>		
17. DISTRIBUTION STATEMENT (of the abstract entered in Block 20, if different from Report)		
18. SUPPLEMENTARY NOTES		
19. KEY WORDS (Continue on reverse side if necessary and identify by block number) <b>Side-scan sonar                      Non-linear acoustics</b> <b>Shoal detection                      Parametric sonar</b> <b>Navigation hazards</b>		
20. ABSTRACT (Continue on reverse side if necessary and identify by block number)  <p>A towed side-scan sonar with 2 nautical mile (nm) range would permit a hydrographic survey ship to sweep a 4 nm swath for navigation hazards. The increased track spacing made possible by such a system would result in substantial savings in ship time.</p> <p>A conical, rather than a fan-shaped, beam would be required in coastal waters because of the proximity of the ocean surface and floor relative to the</p>		

DD FORM 1 JAN 73 1473

EDITION OF 1 NOV 65 IS OBSOLETE  
S/N 0102-LF-014-6601

UNCLASSIFIED

SECURITY CLASSIFICATION OF THIS PAGE (When Data Entered)

**UNCLASSIFIED**

SECURITY CLASSIFICATION OF THIS PAGE (When Data Entered)

sonar range. For isovelocity water with sufficient wave height to make insonification of the surface undesirable, a  $2.5^\circ$  beam would be required for a 2 nm range in 80 meter (m) deep water, or for a 1 nm range in 50 m deep water.

The water depth required under refracting conditions depends on the mixed layer sound speed gradient and the surface wave height.

Nonlinear acoustics can be used to generate the required narrow beams at frequencies compatible with the 2 nm range without the use of excessively large projectors.

A feasibility demonstration experiment was performed at Seneca Lake under isothermal conditions. A transducer with a 0.9 m aperture was rotated in azimuth and excited parametrically in the 13-20 kHz region. Side-scan sonar imagery could be obtained to a range of 3.8 nm. Large features, such as shorelines, points, and underwater ridges, showed up best with 10 millisecond CW pulses. Small features such as sand steps and manmade objects showed up best with replica correlation signal processing.

**UNCLASSIFIED**

SECURITY CLASSIFICATION OF THIS PAGE (When Data Entered)

DATE  
FILME  
7-8